A FINITE ELEMENT ANALYSIS OF PINION SHAPED SPUR GEAR TEETH

by

EDWARD W. RHOMBERG

Thesis submitted to the Faculty of
Virginia Polytechnic Institute and State University
in partial fulfillment of the requirements for the degree of

MASTER OF SCIENCE

in

Mechanical Engineering

APPROVED

R. G. Mitchiner, Chairman

H. H. Mabie

C . E. Knight

November, 1984
Blacksburg, VA

A Finite Element Analysis of Pinion Shaped External Spur Gear Teeth

by

Edward W. Rhomberg

(Abstract)

An analysis of the effects of gear shaping with a pinion cutter upon the geometry and root stresses in external spur gears using the finite element method is given. The models analyzed have the shape of a ring with three teeth. The middle tooth is loaded and load sharing has been assumed. Thirty-five finite element models were used for the computation of stress concentration factors in pinion shaped gear teeth. The results for pinion shaped teeth are compared to those results obtained when shaping with a hob. The Dolan and Broghamer stress concentration factor was also calculated for comparison with the results from finite element analysis. The difference in the two was not more than 8%. The results from finite element analysis have been condensed into an empirical expression which gives the stress concentration factor as a function of the dedendum of the pinion, the numbers of teeth on the pinion and cutter, and the number of teeth on the mating gear. A comparison of the bending stress in the root of a tooth shaped by standard pinion and hob cutters indicated no appreciable differences in strength.

Acknowledgements

The author wishes to extend his thanks to Dr. R. G. Mitchiner for his continual advice and help during the course of this research. He would also like to thank Dr. H. H. Mabie and Dr. C. E. Knight for their advice and guidance and their service on the Graduate Committee.

Nomenclature

a	addendum
b	dedendum
h	height of load above Lewis point
r_c	pitch radius of cutter
r	radius of curvature of fillet at intersection with root circle
t	tooth thickness at Lewis point
x_A, y_A	coordinates of point A on the involute
x_B, y_B	coordinates of point B on the root
x_D, y_D	coordinates of points along the addendum circle
x_L, y_L	coordinates of the Lewis point
x_R, y_R	coordinates of point along the root circle
w	tangential load
w_r	radial load
J	AGMA Geometry factor
K	stress concentration factor
K_D	Dolan & Broghamer Stress concentration factor
K_j	Jalilvand stress concentration factor
K_R	stress concentration factor from regression
N_c	number of teeth on the pinion cutter
N_m	number of teeth on the mating gear
N_p	number of teeth on the cut pinion
P	diametral pitch

Nomenclature

a	addendum
b	dedendum
h	height of load above Lewis point
r_c	pitch radius of cutter
r	radius of curvature of fillet at intersection with root circle
t	tooth thickness at Lewis point
x_A, y_A	coordinates of point A on the involute
x_B, y_B	coordinates of point B on the root
x_D, y_D	coordinates of points along the addendum circle
x_L, y_L	coordinates of the Lewis point
x_R, y_R	coordinates of point along the root circle
w	tangential load
w_r	radial load
J	AGMA Geometry factor
K	stress concentration factor
K_D	Dolan & Broghamer Stress concentration factor
K_j	Jalilvand stress concentration factor
K_R	stress concentration factor from regression
N_c	number of teeth on the pinion cutter
N_m	number of teeth on the mating gear
N_p	number of teeth on the cut pinion
P	diametral pitch
R_α	radius at angle α

R_c radius at intersection if load line and tooth centerline

R_2 pitch radius of mating gear

R pitch radius of cut gear

R_{o2} addendum radius of mating gear

R_x construction line

Q construction line

S_C maximum compressive stress

S_L stress at Lewis point

S_R direct radial stress

S_T maximum tensile stress

α pressure angle at some radius

β angle between centerlines of tooth and space

γ pressure angle at addendum

ξ construction angle

η construction angle

η_e, ξ_e isoparametric element coordinates

θ parameter

κ construction angle

δ construction angle

ϕ cutting pressure angle

ϕ_A pressure angle at addendum

ϕ_L pressure angle at load point

σ combined stress at Lewis point

χ parameter

ω construction angle

Table of Contents

List of Figures

List of Tables

Chapter 1

Introduction

The method of manufacture of external spur gears determines the tooth geometry and many of the resulting characteristics of the gear. Several methods include casting, milling with a form cutter, and shaping with a generating cutter. The casting and milling methods are used when inexpensive less accurate teeth are acceptable. However, when high strength, accurate teeth are desired, shaping with a generating cutter is the preferred method.

A generating cutter may take either the form of a pinion or a rack. A pinion cutter is very similar to a typical involute gear except the teeth have a longer addendum in order to cut the clearence. A rack cutter is a portion of a pinion cutter with an infinite number of teeth.

The geometry and strength of external spur gear teeth that have been shaped with a pinion cutter will be the focus of this study. Comparisons will also be made to those gear teeth that have been generated by a rack cutter.

Many investigations have been conducted to relate stresses in the root of the tooth to the tooth geometry. Shigley [1] presents the method of Wilfred Lewis who inscribed a parabola with in the tooth profile and modeled the tooth as a parabolic cantilever beam. The Lewis method has been incorporated into the American Gear Manufactures Association (AGMA) [2] design standards and is still the basis for most current designs.

The ever increasing demand for improved performance of gear trains operating at higher speeds under larger loads has necessitated the use of more accurate analyses. This need has been met in part by the use of the finite element method and the use of the high-speed digital computer.

To relate stresses in the root of the tooth to its geometry using the finite element method, it was necessary to analyze a range of models. These models were chosen such that undercutting would be avoided, but were also chosen with fewer teeth than the minimum number to avoid undercutting in hobbed teeth. To define the geometry for finite element analysis, first it was necessary to analytically describe all points along the tooth profile. Chapter 3 treats such a development.

Supertab [3] and Superb [4] are two computer programs which are used to generate and analyze the various gear models. Chapter 4 discusses the techniques used in such modeling.

Chapter 2

Literature Review

Shigley [1] states that one of the earliest attempts to analyze the bending strength of external spur gear teeth was that of Wilfred Lewis in 1892. Lewis presented a formula for computing the bending stress in gear teeth. Lewis inscribed a parabola tangent to the root within the tooth profile and intersecting the tooth centerline where the line of action crossed the tooth centerline to represent a parabolic cantilever beam. The point of tangency of the parabola to the tooth root became the critical stress point. Dimensions of the beam were determined graphically from a layout of the tooth, parabola, and the load line.

In 1942, Dolan and Broghamer [5] used photoelastic techniques to analyze bending stresses developed in the roots of spur gear teeth. From their results, Dolan and Broghamer concluded that the location of the maximum stress obtained was not greatly different than the location determined by Lewis. Dolan and Broghamer applied the load to the flank of the tooth consistent with that load the tooth would be subjected to when engaging a mating gear, but simplied the root form by assuming a fillet of constant curvature. Dolan and Broghamer used the Lewis beam theory to compute the nominal stress at the root, then condensed their results into two equations which gave the stress conentration factor K_d as:

for a 14.5 degree pressure angle

$$K_D = .22 + \left(\frac{t}{r}\right)^{.2} \cdot \left(\frac{t}{h}\right)^{.45}$$

for a 20^o degree pressure angle

$$K_D = .13 + \left(\frac{t}{r}\right)^{.15} \cdot \left(\frac{t}{h}\right)^{.45}$$

The work of Lewis, and Dolan and Broghamer has become the standard for design in the American Gear Manufactures Association (AGMA) [2]. AGMA presents several methods to assess the bending strength of a gear. The first method is a graphical procedure to determine the necessary dimensions for use in the Lewis and Dolan and Broghamer formulae. The second method is the use of charts to obtain the geometry factor which can be then used to determine the intensity of the bending stress. The geometry factor is the quotient of the Lewis factor and the Dolan and Broghamer stress concentration factor. The use of the graphical method is difficult to implement and is also inaccurate because the root form is often simplified. The chart method is limited to only standard hob shaped gear teeth. Charts for pinion-shaped teeth are not presented. A third method is presented which discusses an analytical determination of the Lewis factor for hobbed teeth. No method is given to determine the Lewis factor for pinion-shaped teeth.

Chang, Huston, and Coy [6] performed a finite element analysis of spur gear teeth to investigate the effects of fillet radii upon the

maximum stress. These authors noted that the maximum stress increased for decreasing radius of curvature in the fillet. No mention was made as to the method of cutting or generating.

Chabert, Tran, and Mathis [7] also used finite elements in plane elasticity and applied them to spur gears. Their resulting stress concentration factors were also in substantial agreement with those of Dolan and Broghamer [5].

In 1974, Winter and Hirt [8] measured actual strains in gear tooth fillets with miniature foil strain gages. Gears with varying fillet radii were tested. Their results compared favorably with the photoelastic results obtained by Dolan and Broghamer [5].

Shotter [9] offered an alternate isotropic wedge theory based upon the Airy stress function. Shotter claimed the conventional beam bending approach was not adequate for teeth of low height. Shotter concluded, however, that even his theory could not provide information for root failures and that a finite element stress analysis was necessary to provide proper stress information around the root surface.

Wilcox and Coleman [10] used the finite element method to determine the maximum stress in gear tooth fillets. They inscribed small quadrilateral elements within the boundaries of tooth profiles that were generated by a hob. Wilcox and Coleman expressed their results in a semi-empirical formula that gave the tensile fillet stress as a function of tooth geometry and general loading conditions.

Baronet and Tordion [11] used the two-dimensional theory of elasticity and an appropriate transform function to obtain the stress

distribution in a gear tooth acted on by a concentrated load. Baronet and Tordion considered teeth cut with a finishing hob, for 20^{o} and 25^{o} pressure angles. Their results were expressed in the form of a dimensionless factor J which was compared to the AGMA geometry factor J. Baronet and Tordion found good agreement for the case of tip loading but differed appreciably for loading positions closer to the pitch point.

Aida and Teruchi [12] also used two-dimensional theory of elasticity and the transform function to compute fillet stresses. Aida and Teruchi found that the distribution of stress in the weakest section has almost the same tendency as the nominal stress, but it causes a stress concentration on the fillet curve. Their results were in good agreement with those of Dolan and Broghamer [5].

Jalilvand [13] used the finite element method to investigate the effects of undercutting in hobbed spur gear teeth. Jalilvand validated his work by analyzing the Dolan and Broghamer [5] photoelactic model. The author's results compared well with those of Dolan and Broghamer.

Mitchiner and Mabie [14] present a method for the numerical computation of the Lewis form factor and stress for hobbed spur gear teeth. A similar procedure will be used subsequently for computing the Lewis form factor and stress for pinion-shaped teeth.

The focus of most treatments hitherto has been on gear teeth with simplified root forms or those obtained when using a hob. After reviewing the literature it was noted that no investigations of pinion shaped teeth were performed.

Chapter 3

The Geometry of Pinion-Shaped Gear Teeth

3.1 Introduction

This chapter presents the geometry of pinion-shaped gear teeth. Derivation of parametric equations defining the tooth root, flank and top land profiles are given. The finite element models used later are based upon the geometry developed herein.

3.2 Development of Root Form

The process of generating the root form on an external spur gear tooth may be visualized and analyzed as that of rolling a pinion cutter around a stationary blank, with no slippage on the tangent cutting pitch circles.

Consider first, one cylinder rolling around another as shown in Figure 3.1. Circle Δ rolls without slipping around stationary circle Γ. Point E traces the path of a plane curve known as an epicycloid. In the fixed global coordinate system, the x and y coordinates of points along this curve are given by

$$X_E = (R + r)\sin\chi - r\sin\left(\chi\left(\frac{R + r}{r}\right)\right) \tag{3.1}$$

$$Y_E = (R + r)\cos\chi - r\cos\left(\chi\left(\frac{R + r}{r}\right)\right) \tag{3.2}$$

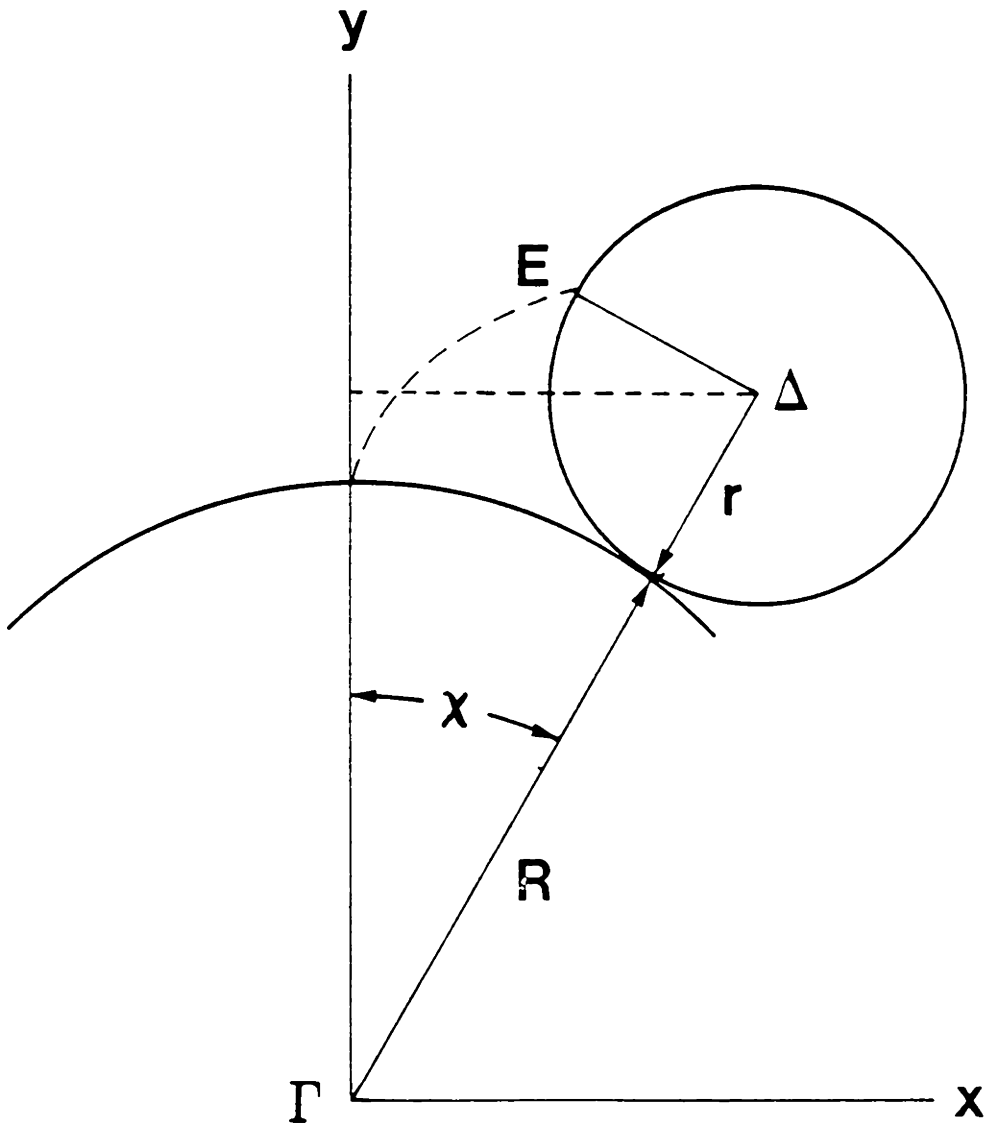

Fig. 3.1 One cylinder rolling on another

Next consider the arrangement shown in Figure 3.2. The smaller portion of a gear is the the cutter and the larger is the blank. As the cutter rolls around the blank, it shapes the tooth profile. Generation of the tooth root begins when Line C of the pinion cutter is colinear with Line J of the blank. As the pitch surface of the cutter is rolled about the pitch surface of the blank, Point B the corner of the cutter tooth, shapes the resulting root profile. For gears generated by pinion cutters, it is the corner of the cutter tooth that solely determines the root. In practice, as the tool wears, the corner would become rounded, but typically the tool is sharpened frequently such that there are no appreciable differences. Generation of the root ceases when the cutter has rolled such that Point B lies outside the involute tooth flank. The path which Point B traces in known as a curtate epitrochoid.

The preceeding parametric equations (3.1) and (3.2) describing a generalized epicycloid curve may be specialized to describe the root profile on a gear blank when it is generated by a pinion cutter. The path traveled by the corner of the tool becomes the root on the resulting gear. The following equations are valid only for sharp-cornered pinion cutters. From Figure 3.2, the coordinates of points along the root profile of the gear are determined to be:

$$X_B = (R + r_c)\sin(\beta + \theta) - (r_c + a)\sin\left(\theta\left(\frac{R + r_c}{r_c}\right) + \beta + \eta\right) \quad (3.3)$$

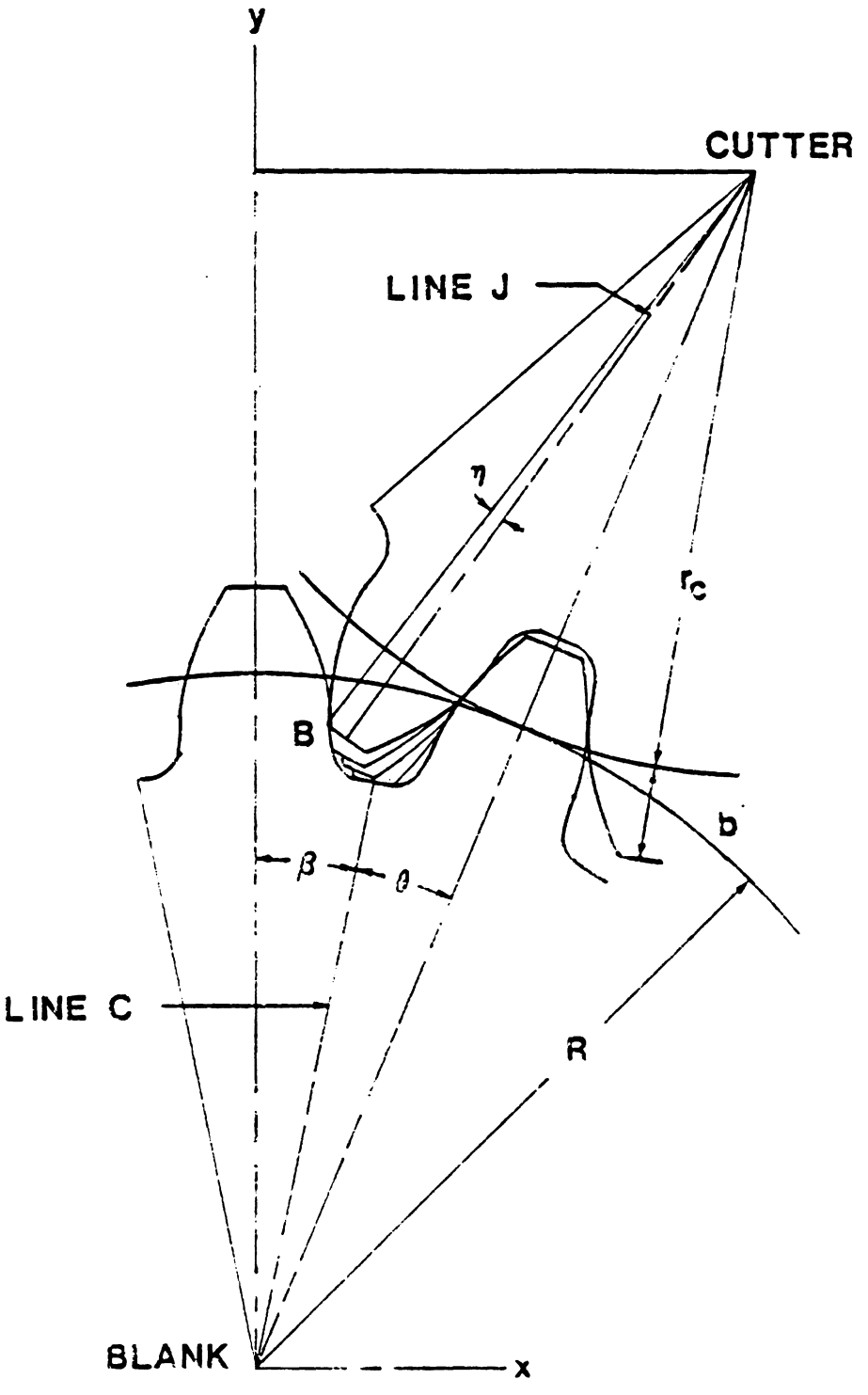

Fig. 3.2 Pinion cutter shaping a blank

$$Y_B = (R + r_c)\cos(\beta + \theta) - (r_c + a)\cos\left(\theta\left(\frac{R + r_c}{r_c}\right) + \beta + \eta\right) \quad (3.4)$$

where θ is the angle between the centerline of the space on the blank and the line between the centers of the cutter and blank, and where β, the angle between the blank tooth centerline and space center, is

$$\beta = \frac{\pi}{N} \quad (3.5)$$

and where η, the angle between the cutter-tooth centerline and tooth corner, is

$$\eta = \frac{\eta}{2N} + \text{inv } \phi - \text{inv } \phi_A \quad (3.6)$$

3.3 Tooth Flank Profile

In defining the geometry, it was necessary to derive parametric equations to describe the involute portion of the tooth. Figure 3.3 shows a half tooth with its pitch and base circles. Point A is some point along the flank and angle AOC is equal to

$$AOC = \frac{P}{2R} + \text{inv } \phi - \text{inv } \alpha \quad (3.7)$$

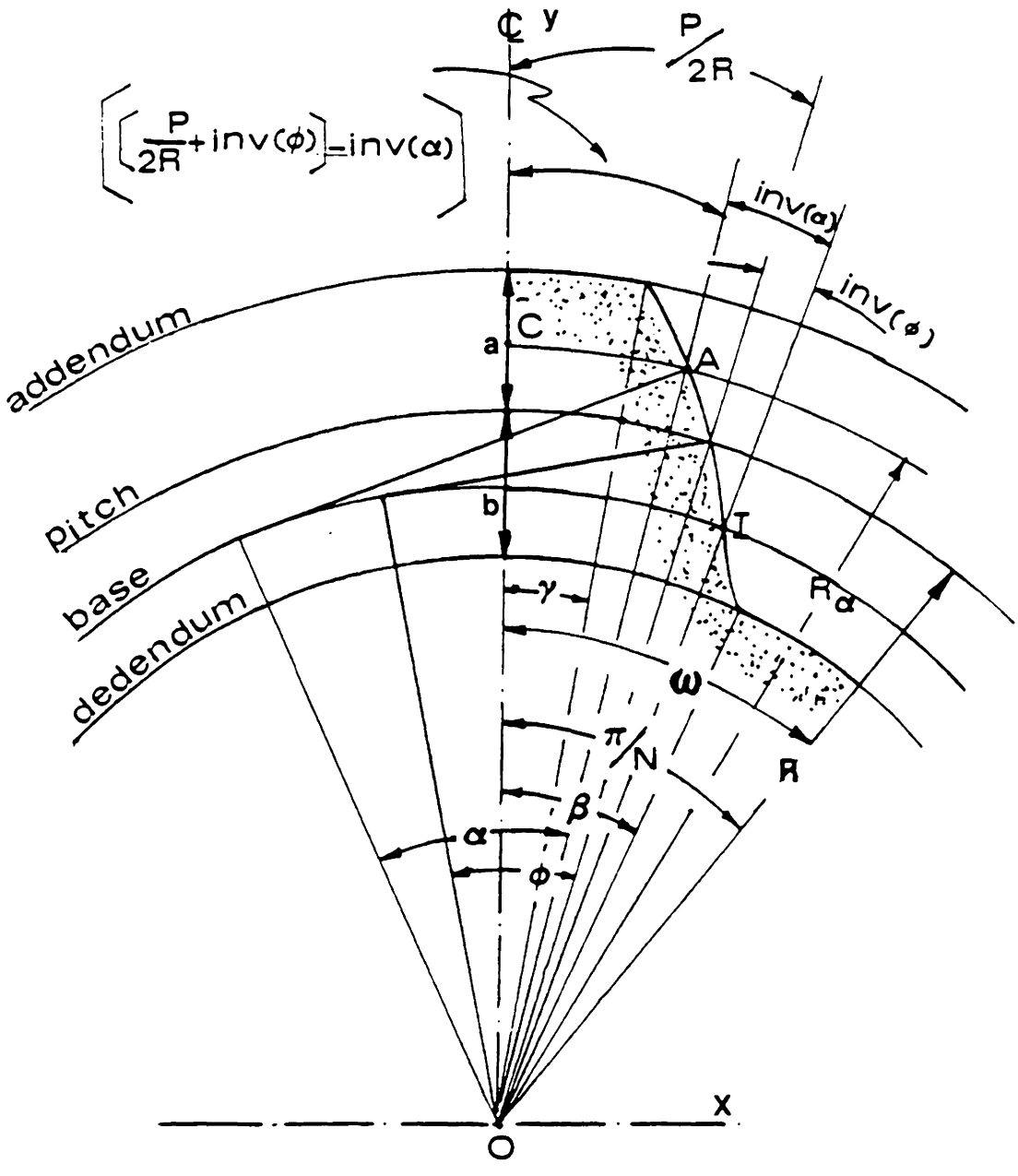

Fig. 3.3 Generation of tooth profile

and

$$R_{\alpha} = \frac{R \cos\phi}{\cos\alpha} \tag{3.8}$$

From Figure 3.3 the coordinates of the involute are determined to be:

$$x_A = R_{\alpha} \sin(AOC) \tag{3.9}$$

$$y_A = R_{\alpha} \cos(AOC) \tag{3.10}$$

then substituting (3.8)

$$x_A = \frac{R \cos\phi}{\cos\alpha} \cdot \sin(\frac{P}{2R} + \text{inv } \phi - \text{inv } \alpha) \tag{3.11}$$

$$y_A = \frac{R \cos\phi}{\cos\alpha} \cdot \cos(\frac{P}{2R} + \text{inv } \phi - \text{inv } \alpha) \tag{3.12}$$

Coordinates of points along the root circle are determined from Figure 3.3 to be:

$$x_R = (R - b) \sin\omega \tag{3.13}$$

$$y_R = (R - b) \cos\omega \tag{3.14}$$

Similarly, coordinates of points along the addendum circle are determined to be:

$$y_D = (R + a) \sin\gamma \tag{3.15}$$

$$y_D = (R + a) \cos\gamma \tag{3.16}$$

3.4 Tooth Profile Program

The equations developed in the preceeding sections to define the tooth geometry were incorporated into subroutines that were added to the main program in Ref. [13]. This program may be found in Appendix A. The computer program first computes the coordinates of points along the root circle using equations (3.13) and (3.14) for ω from π/N to β .

Next, coordinates of points along the root are computed using equations (3.3) and (3.4) for θ from 0 to the value of θ at the intersection of the root and the involute flank. The value of θ at the intersection is found by solving equations (3.3), (3.4), (3.11), and (3.12) simultaneously for θ and α. This is accomplished numerically by using finite differences to approximate the derivatives and a Newton-Raphson scheme to compute the roots.

Then coordinates of points along the involute are calculated for values of α at the intersection point to α equal to ϕ_A where

$$\phi_A = \cos^{-1}\left(\frac{R \cos\phi}{R + a}\right) \tag{3.17}$$

Lastly, equations (3.15) and (3.16) are used in computing coordinates of points on the addendum circle where

$$0 < \gamma < \left(\frac{P}{2R} + \text{inv } \phi - \text{inv } \phi_A\right)$$

After computing coordinates of points on the tooth profile, the data could then be recorded in a file, to be used later for geometry definition in finte element modeling.

Chapter 4

Finite Element Modeling and Analysis

4.1 Introduction

This chapter presents an explanation of the finite element method and the basis for its use. Modeling techniques are given as well as a method for calculating the theoretical beam stress. Lastly, a description of the thirty-five models analyzed is presented.

4.2 Validity of the Finite Element Method

Jalilvand [13] performed a finite element analysis of undercut external spur gear teeth. In order to validate his work, Jalilvand correlated his results with those obtained by Dolan and Broghamer [5]. Dolan and Broghamer obtained real stress distributions in gear teeth fillets utilizing the photoelastic technique. Jalilvand simulated the Dolan and Broghamer experiment using a finite element model. He was able to agree within 1.5% of Dolan and Broghamer's findings. Consequently, this research will employ the finite element method based upon Jalilvand's findings and recommendations.

4.3 SUPERTAB

SUPERTAB [3] is a state-of-the-art computer program that allows the user to prepare data for finite element analysis. SUPERTAB is a product of General Electric CAE International Inc.

After the definition of the tooth profile, a model was created by joining arcs, splines, and lines created in the program in Appendix A.

The next step was to discretize the domain by using enhanced mesh generation in SUPERTAB. In enhanced mesh generation, elements and nodes are automatically generated, thus sparing the user from the demands of laying out a mesh. The user may control the mesh density. For the case of a tooth loaded on its flank by a concentrated force, it was necessary to have a finer mesh in the vicinity of the load, such that the load could be applied in the proper location. It was also necessary to have a relatively fine mesh in the root at the tooth where the stress gradients would be the largest. Based upon conclusions drawn by Jalilvand [13], a local element length of .010 was chosen as a starting mesh size in the root for teeth with a diametral pitch of unity. This local element length was obtained by prescribing a number of elements along the root. After successive trials, the number of elements along the root was obtained for which the finite element method had satisfactorily converged. Figure 4.1 shows a finite element model of a tooth.

SUPERTAB allows the user to input material properties, boundary conditions, and other loads such as pressures. Appendix B contains a SUPERTAB PROGRAM FILE, and a log of all the commands used in the creation of a finite element model. After all input data was processed, a file for Superb analysis was written.

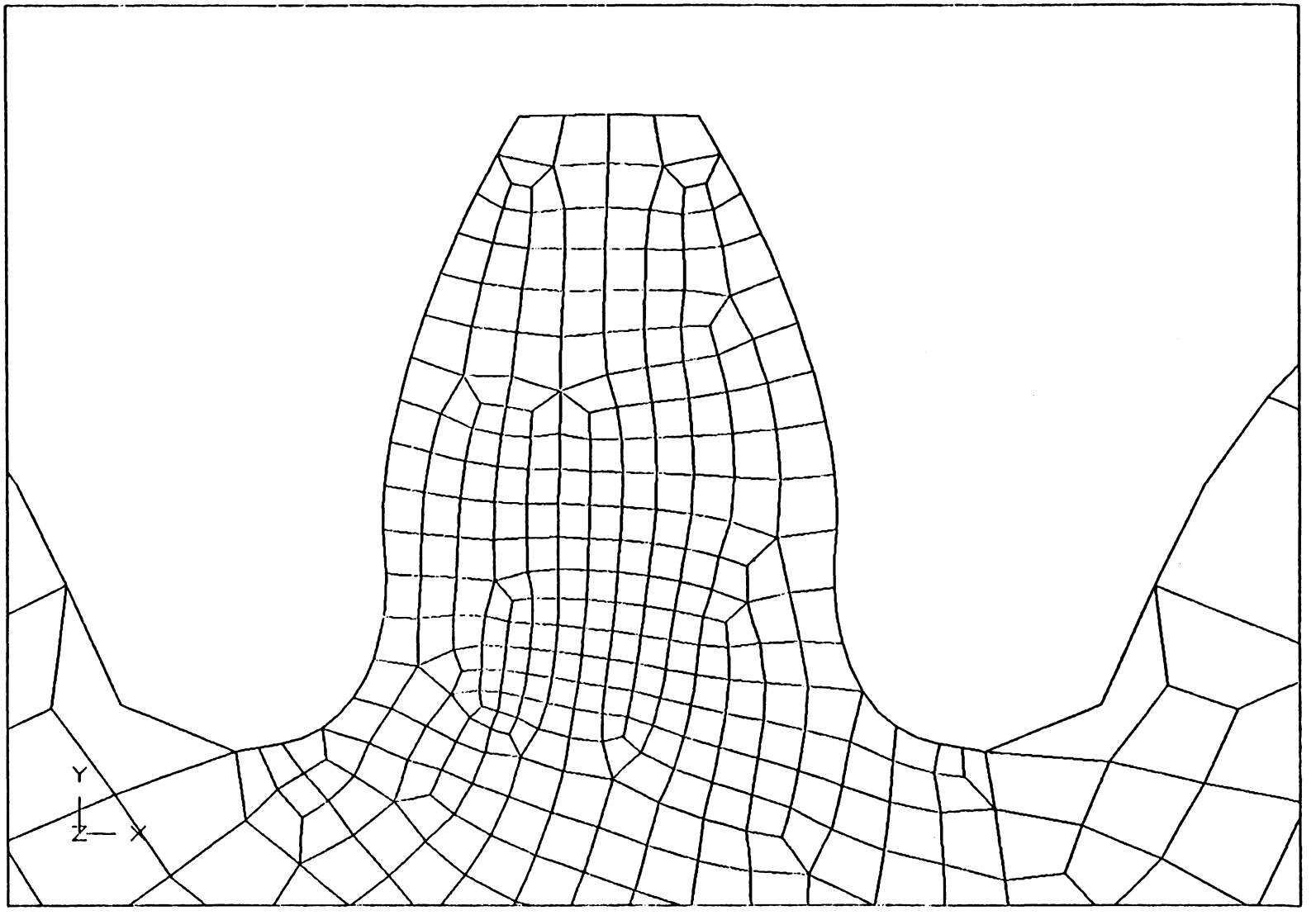

Fig. 4.1 Finite element model of a tooth

4.4 SUPERB

SUPERB [4], another product of GE/CAE, is a program which accepts the input data created in SUPERTAB, then performs the finite element analysis. The finite element method is a technique used to analyze structural behavior where an exact solution is not possible, such as the case with a spur gear and its complicated geometry. In the finite element method, a given physical domain is approximated by a finite number of assembled elements whose structural behavior is known. With the elements assembled, a system of equations for equilibrium may be formulated, solved and results obtained.

In this analysis, the tooth was modeled as an assembly of plane stress elements. Stresses normal to the plane of the tooth were neglected. Quadratic plane isoparametric elements were chosen to better model the curved boundaries and to more accurately approximate the displacements. After solving the system of equations for the nodal displacements, strains were computed, then the nodal stresses. The nodal stress is actually an extrapolation of the stress from the elemental Gauss points. In the isoparametric element formulation, the stresses are obtained through numerical integration using Gauss quadrature. It has been found that the stresses are most accurate when computed at the integration points or Gauss points. Later it will be shown that the nodal stresses obtained have been accurately extrapolated from the Gauss points.

4.5 Modeling

Jalilvand [13] investigated several types of gear models. Jalilvand noted that a whole gear model produced the most reliable results in comparision to the Dolan and Broghamer model and a three tooth wedge model. The whole gear model is a ring of unit depth that has three teeth. In the case of load sharing, only one tooth carries the load, however, and the two adjacent teeth are necessary to model the interaction between the three teeth. Load sharing will be discussed subsequently. This research also used three tooth whole gear models.

Jalilvand [13] also considered the effect of the bore of the gear. Jalilvand noted that pitch to hole diameter ratios of two or more had little effect on the maximum stress in the root. Therefore, this research used a pitch to hole diameter ratio of two in all models.

After defining the geometry for a finite element model, boundary conditions were imposed and loads applied. In this research, all nodes along the hole of the three tooth gear model were restrained in two directions in the plane of loading.

4.6 Loading the Tooth to Produce the Largest Principal Stress

It was necessary to apply a concentrated force to a point on the tooth flank that would be consistant with the force transmitted to the tooth from a mating gear. The location of this point depended upon whether load sharing existed. In the case of load sharing, (i.e., a contact ratio greater than unity) more than one pair of teeth are in contact for a portion of tooth movement along the length of action. The

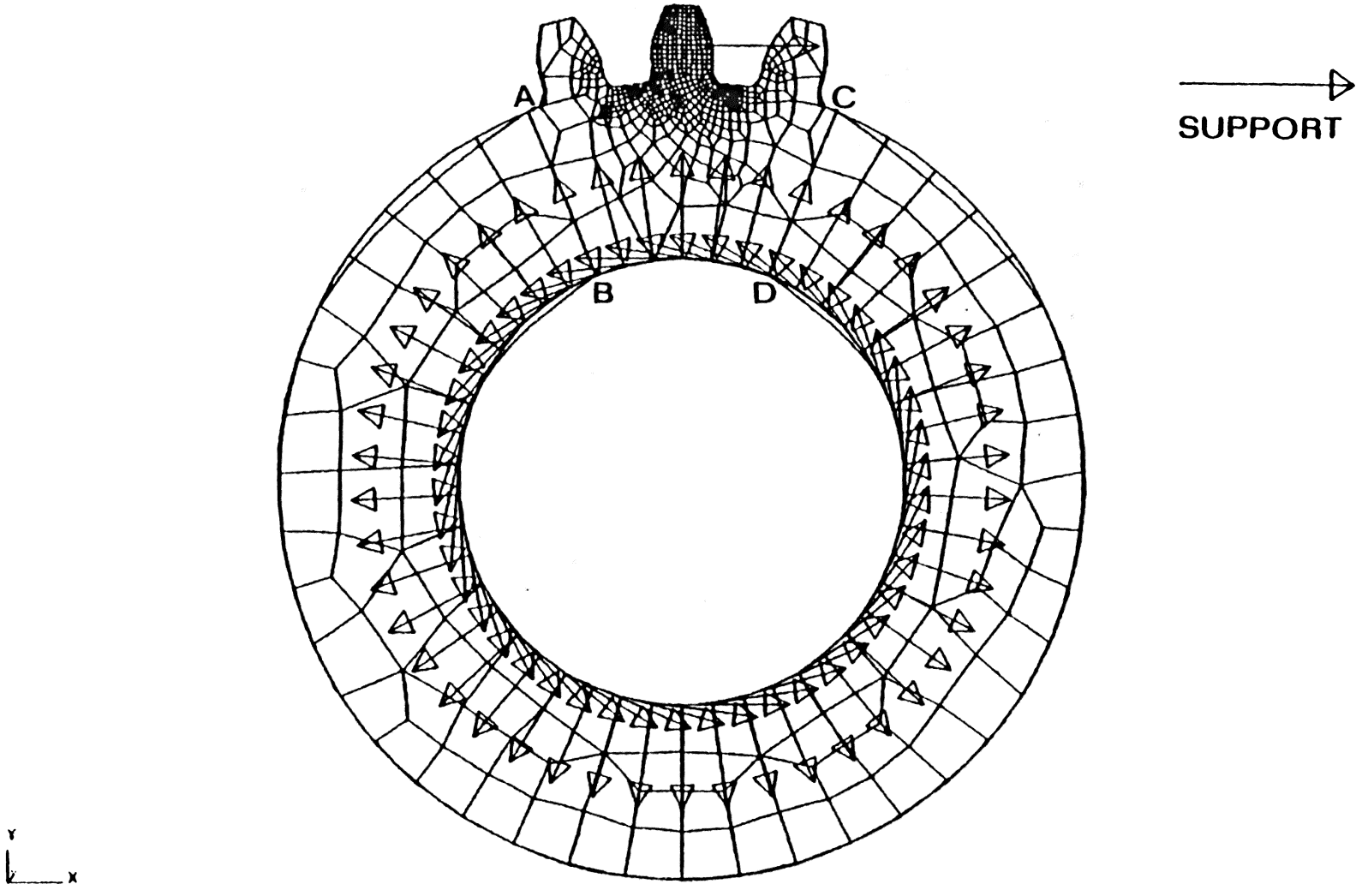

Fig. 4.2 Whole gear finite element model.

worst case occurs when one of the pairs of mating teeth has just left contact, leaving only one pair of teeth to carry the load as shown in Figure 4.3. Mitchiner and Mabie [14] have defined Point U in Figure 4.3 as the farthest point from the root at the intersection of load line and the tooth centerline. These authors have expressed the distance R_c between Point U and the center of the gear as follows:

$$R_{o2} = R_2 + a \tag{4.1}$$

$$\tau = \sin^{-1} \frac{R_2 \cos\phi}{R_{o2}} \tag{4.2}$$

$$R_x = \sqrt{Q^2 + R_1^2 - 2\,Q\,R_1 \sin\phi} \tag{4.3}$$

where

$$Q = \frac{\cos(\tau + \phi)\, R_2}{\sin\tau} \tag{4.4}$$

$$\kappa = \frac{\pi}{2N} - \text{inv}\left(\cos^{-1} \frac{R_1 \cos\phi}{R_\alpha}\right) + \text{inv}\ \phi \tag{4.5}$$

$$\xi = \frac{2\tau}{N} - \kappa \tag{4.6}$$

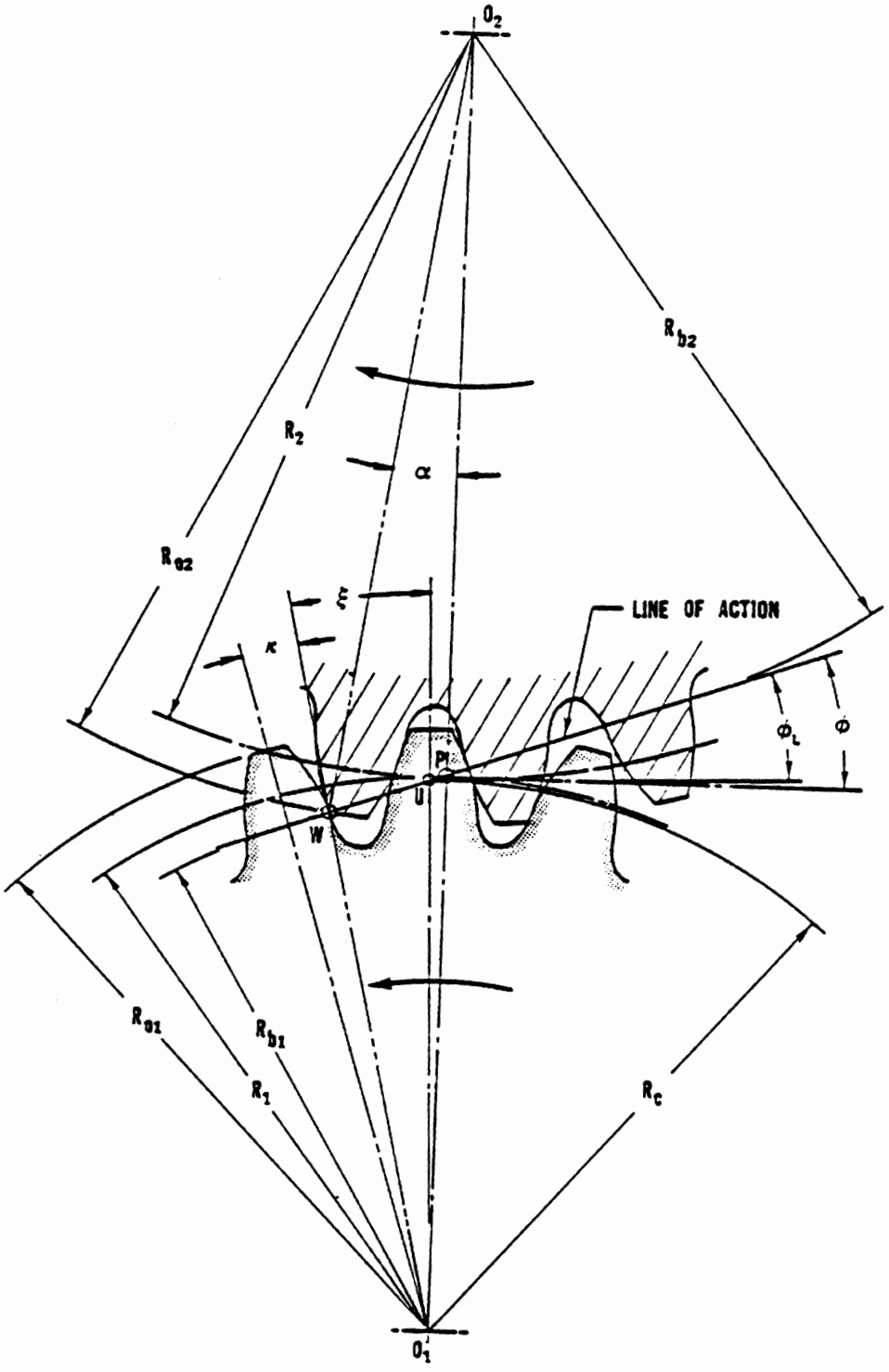

Fig. 4.3 Load at highest point for single-tooth contact [14]

$$\zeta = \cos^{-1}\left[\frac{R_x^2 + R_{02}^2 - (R_1 + R_2)^2}{2 R_x R_{02}}\right] - \tau \qquad (4.7)$$

finally

$$R_c = \frac{R_x \sin(\zeta)}{\sin(\zeta + \xi)} \qquad (4.8)$$

ϕ_L, the angle between the load line and the horizontal, is given by:

$$\phi_2 = \tan^{-1}\left[\frac{\sqrt{1 - \left(\frac{R\cos\phi}{(R+a)}\right)^2}}{\frac{R\cos\phi}{(R+a)}}\right] - \frac{\pi}{2N}$$

$$- \text{inv}\left[\frac{\tan^{-1}\sqrt{1 - \left(\frac{R\cos\phi}{(R+a)}\right)^2}}{\frac{R\cos\phi}{(R+a)}}\right] + \text{inv}\,\phi \qquad (4.9)$$

In all of the finite element models analyzed, a unit load was applied to a node lying on or near the line passing through Point U at an angle ϕ_L. This force is consistent in direction with the transmitted load from a mating gear. In this study, the number of teeth on the

mating gear has been set at twenty. A special study will be conducted to determine the influence of the relative size of the mating gear upon the strength of the pinion. The relative size of a mating gear only affects the position of the load applied to the model.

4.7 Stress at the Lewis Point

For the purpose of computing stress concentration factors, the cantilever beam stress at the Lewis point was calculated. The theoretical weakest location is the point of tangency of a parabola inscribed in the tooth profile with its apex at Point U (Fig. 3.2) and tangent to the root of the tooth.

To locate the Lewis point, a subroutine based upon the procedure outlined in Mitchiner and Mabie [14] was written. This subroutine was then added to the main program in [13]. Using a Newton-Raphson method and finite differences to approximate derivatives, equations (3.3) and (3.4) and (4.8) were used to numerically compute the Lewis point (x_L, y_L). With the coordinates of Point U and the Lewis point, the tensile or compressive flexural stress was determined by means of the Lewis equation:

$$S_L = \frac{6wh}{t^2} \tag{4.10}$$

where h, the distance between the load position and the weakest section, is

$$h = R_c - y_L \tag{4.11}$$

The direct stress S_R due to compression by the applied load was obtained by dividing the radial component of the load, W_r, by the cross-sectional area of the tooth. This stress was then added algebraically to the stress computed from the Lewis equation, to give the combined bending and normal stress σ

$$S_R = \frac{W_R}{t} = \frac{w \tan\phi_L}{t} \tag{4.12}$$

$$\sigma = S_L + S_R = \frac{6wh}{t^2} - \frac{w \tan\phi_L}{t} \tag{4.13}$$

All models analyzed had a face width of unity.

4.8 Description of the Models

Thirty five models were analyzed with the finite element method in order to determine stress concentration factors in spur gear teeth

shaped by a pinion cutter. These models, listed in Table 4.1, have been divided into two principal groups A & B. Group A has a dedendum ratio of 1.2 while Group B has a dedendum ratio of 1.25. Within Groups A & B are four sub-groups each with four models. Each subgroup is a pinion of N number of teeth shaped by four cutters with various numbers of teeth. None of the models are undercut, however the model in each principal group with the fewest number of teeth, has just enough teeth to avoid undercutting.

Table 4.1

Description of Gear Models

$\phi = 20^{o}$ P = 1 a = 1.0 in

MODEL	N_p	N_c	b	N_m
A1	15	13	1.2	20
A2	15	14	1.2	20
A3	15	15	1.2	20
A4	15	16	1.2	20
A5	16	14	1.2	20
A6	16	15	1.2	20
A7	16	16	1.2	20
A8	16	22	1.2	20
A9	18	14	1.2	20
A10	18	16	1.2	20
A11	18	18	1.2	20
A12	18	22	1.2	20
A13	22	14	1.2	20
A14	22	19	1/2	20
A15	22	22	1.2	20
A16	22	26	1.2	20

Table 4.1 continued

MODEL	N_p	N_c	b	N_m
B1	16	13	1.25	20
B2	16	14	1.25	20
B3	16	16	1.25	20
B4	16	18	1.25	20
B5	18	14	1.25	20
B6	18	16	1.25	20
B7	18	18	1.25	20
B8	18	26	1.25	20
B9	21	14	1.25	20
B10	21	16	1.25	20
B11	21	21	1.25	20
B12	21	26	1.25	20
B13	24	14	1.25	20
B14	24	16	1.25	20
B15	24	24	1.25	20
B16	24	28	1.25	20

Chapter 5

After generation of the finite element models with Supertab [3], an analysis was performed. The results of the Superb [4] analysis were recorded in an output file that listed the maximum nodal principal stress, S_T, and minimum nodal principal stress, S_C. In order to ensure that the Gauss point stresses were accurately extrapolated to the boundary nodes, a check was made. Table 5.1 lists the stresses at the Gauss points for the element of a particular model that contained the node with the largest principal stress. Also tabulated are the values of maximum nodal stress that the Superb result indicated, and a value that was extrapolated by hand calculation. Figure 5.1 shows the variation in elemental Gauss point stresses and the stress extrapolated to the boundary. The percentage error was .06%. Hence the nodal stress computed by Superb is considered to be accurately extrapolated to the boundary.

Beam stresses, using

$$\sigma = \frac{6wh}{t^2} - \frac{w \tan\phi_L}{t} \qquad (4.13)$$

were computed for each model. In addition, thirty-five pinion shaped models, and eight hobbed models having identical addenda and dedenda were analyzed for purposes of comparison. Beam stresses using (4.13) were also computed for the hobbed cases.

Table 5.1

Element Gauss point stresses, and boundary extrapolated nodal stress

Gauss Point	η_e	ξ_e	Stress psi
1	.774	.774	2.954
2	0	.774	2.310
3	-.774	.774	1.850
4	.774	0	3.075
5	0	0	2.339
6	-.774	0	1.911
7	.774	-.774	3.077
8	0	-.774	2.330
9	-.774	-.774	1.934

Nodal principal stress in Superb: S_T = 3.346 psi

Nodal stress extrapolated along ξ_e = 0, to η_e = 1 : S_E = 3.348 psi

Percentage error .06%

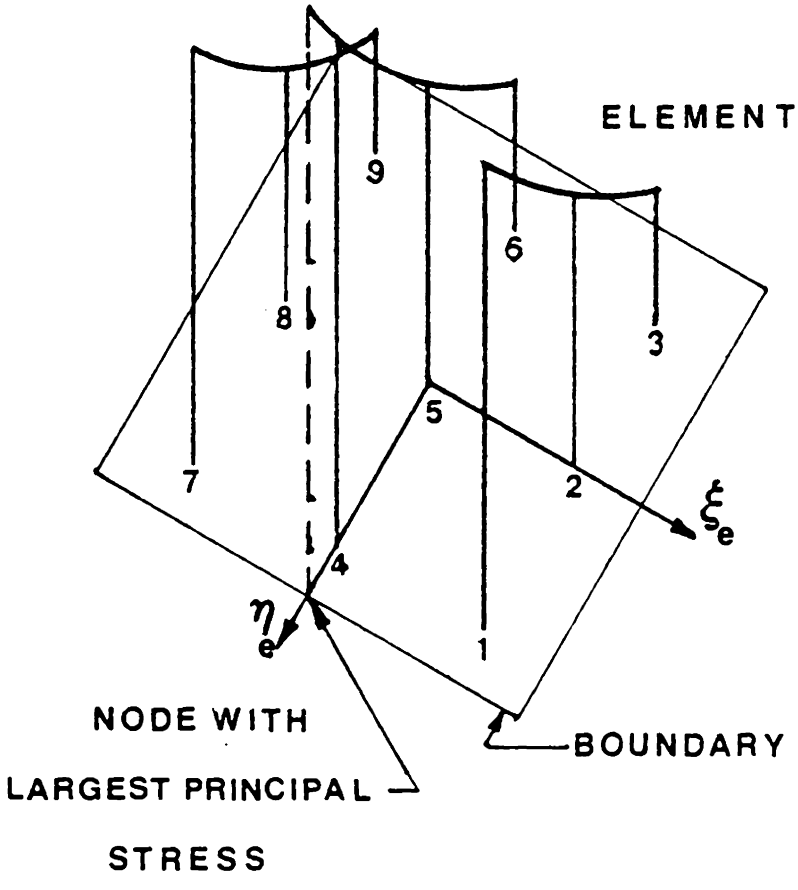

Fig. 5.1 Element with Gauss point stresses and extrapolated nodal stress

The combined tensile stress concentration factor was defined as the quotient of the maximum tensile stress to the combined stress σ.

$$K = \frac{S_T}{\sigma} \tag{5.1}$$

The Dolan and Broghamer [5] equation for stress concentration factors in 20° pressure angle gear teeth is as follows:

$$K_D = .13 + \left(\frac{t}{r}\right)^{.15} \cdot \left(\frac{t}{h}\right)^{.45} \tag{5.2}$$

Table 5.2 presents the results of the Superb analysis as well as stresses computed from equation (4.13) and stress concentration factors determined from (5.1) and (5.2).

Figures 5.2 and 5.3 show the variation in maximum tensile stress of four pinions as a function of the number of cutter teeth. The case of four hobbed pinions has also been included. Figures 5.4 and 5.5 show the variation in stress concentration factor with the number of cutter teeth, as computed from (5.1).

In Figures 5.6 and 5.7 the theoretical combined stress for four pinions is plotted against the number of cutter teeth. The stress due to hobbing is also included.

Table 5.2

Results

Model	σ psi	S_T psi	S_C psi	K FEM	K_D D&B*
A1	1.4821	2.8916	3.4391	1.9510	1.8933
A2	1.4956	2.9396	3.6383	1.9655	1.8926
A3	1.5079	2.9580	3.6550	1.9617	1.8871
A4	1.5193	2.9676	3.6671	1.9537	1.8821
A5	1.4386	2.8784	3.5491	2.0008	1.9297
A6	1.4502	2.8936	3.5516	1.9953	1.9242
A7	1.4609	2.9044	3.6109	1.9881	1.9192
A8	1.5111	3.0565	3.8154	2.0227	1.8936
A9	1.3497	2.7563	3.3946	2.0422	1.9951
A10	1.3699	2.7962	3.4976	2.0432	1.9348
A11	1.3872	2.8495	3.5803	2.0541	1.9766
A12	1.4152	2.9365	3.5711	2.0750	1.9644
A13	1.2333	2.6046	3.2146	2.1119	2.1003
A14	1.2654	2.7279	3.4069	2.1558	2.0821
A15	1.2895	2.8091	3.5567	2.1784	2.0704
A16	1.3032	2.9203	3.5716	2.2323	2.0621

*Dolan & Broghamer

Table 5.2
continued

Model	σ	S_T	S_C	K	K_D
	psi	psi	psi	FEM	D&B*
B1	1.4839	2.7347	3.4636	1.8766	1.9226
B2	1.4976	2.8386	3.4650	1.8954	1.9156
B3	1.5219	2.9829	3.5949	1.9600	1.9041
B4	1.5428	3.0025	3.6752	1.9461	1.8949
B5	1.4012	2.7792	3.4336	1.9334	1.9320
B6	1.4230	2.8430	3.4956	1.9979	1.9705
B7	1.4417	2.8953	3.5546	2.0082	1.9614
B8	1.4961	3.0773	3.8184	2.0569	1.9330
B9	1.3008	2.6594	3.3029	2.0443	2.0650
B10	1.3201	2.6685	3.3945	2.0214	2.0535
B11	1.3573	2.7981	3.5340	2.0615	2.0338
B12	1.3844	2.8519	3.6297	2.1372	2.0214
B13	1.2370	2.5711	3.1479	2.0369	2.1337
B14	1.2495	2.6640	3.3190	2.1321	2.1219
B15	1.2988	2.8072	3.4838	2.1615	2.045
B16	1.3158	2.8792	3.5781	2.1882	2.0366

*Dolan & Broghamer

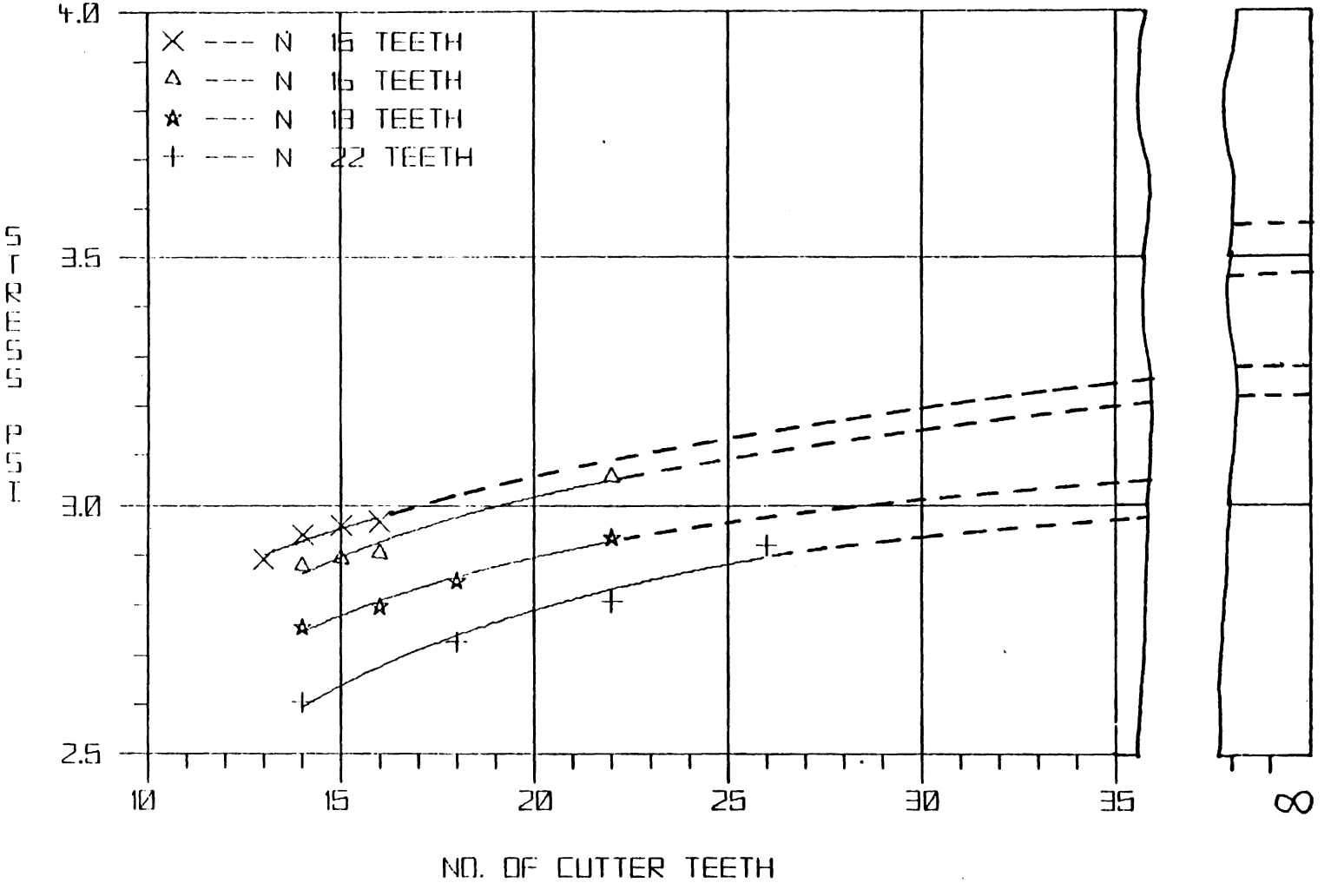

Fig. 5.2 Variation of maximum tensile stress versus the number of cutter teeth (b = 1.2 in)

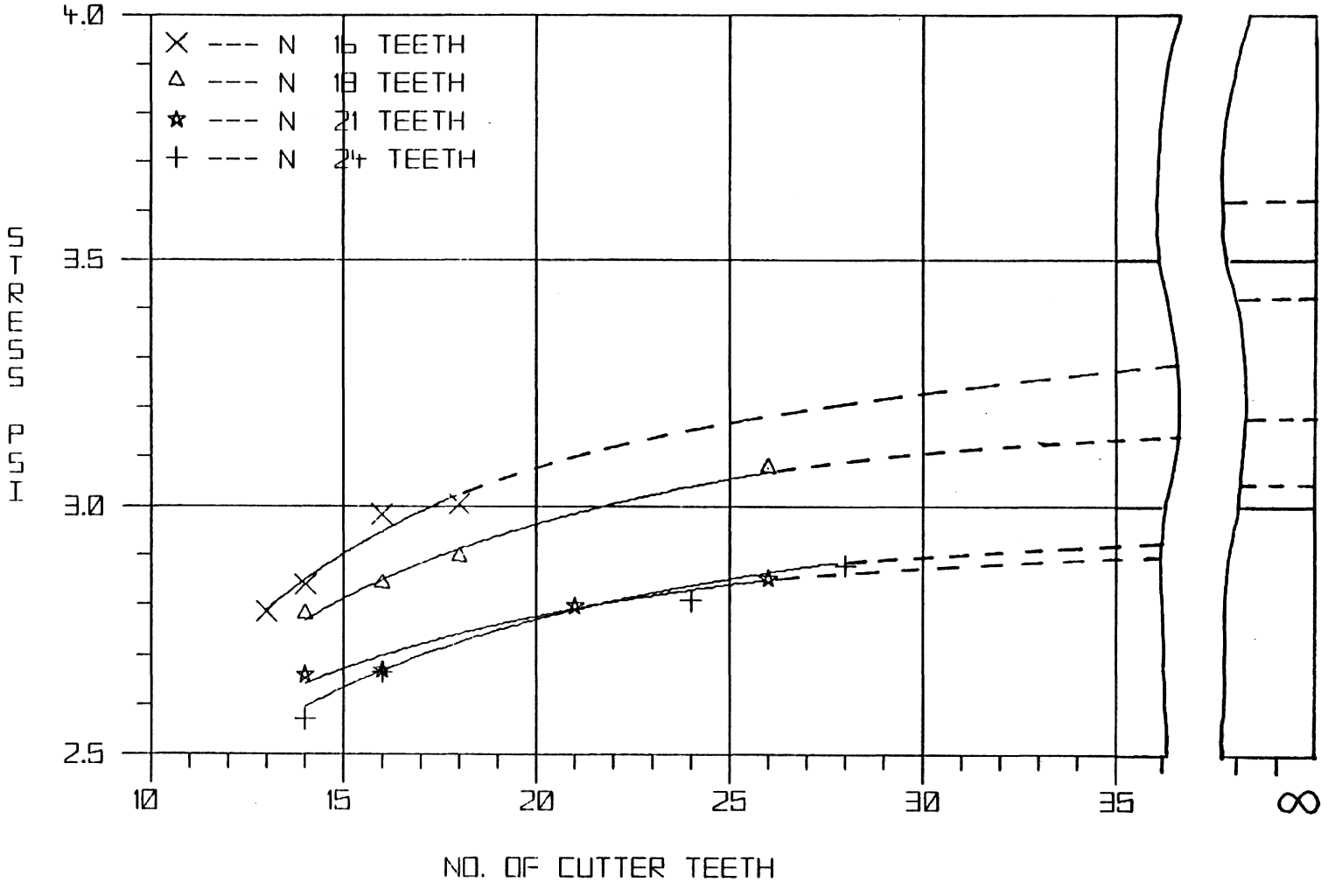

Fig. 5.3 Variation of maximum tensile stress versus the number of cutter teeth (b = 1.25 in)

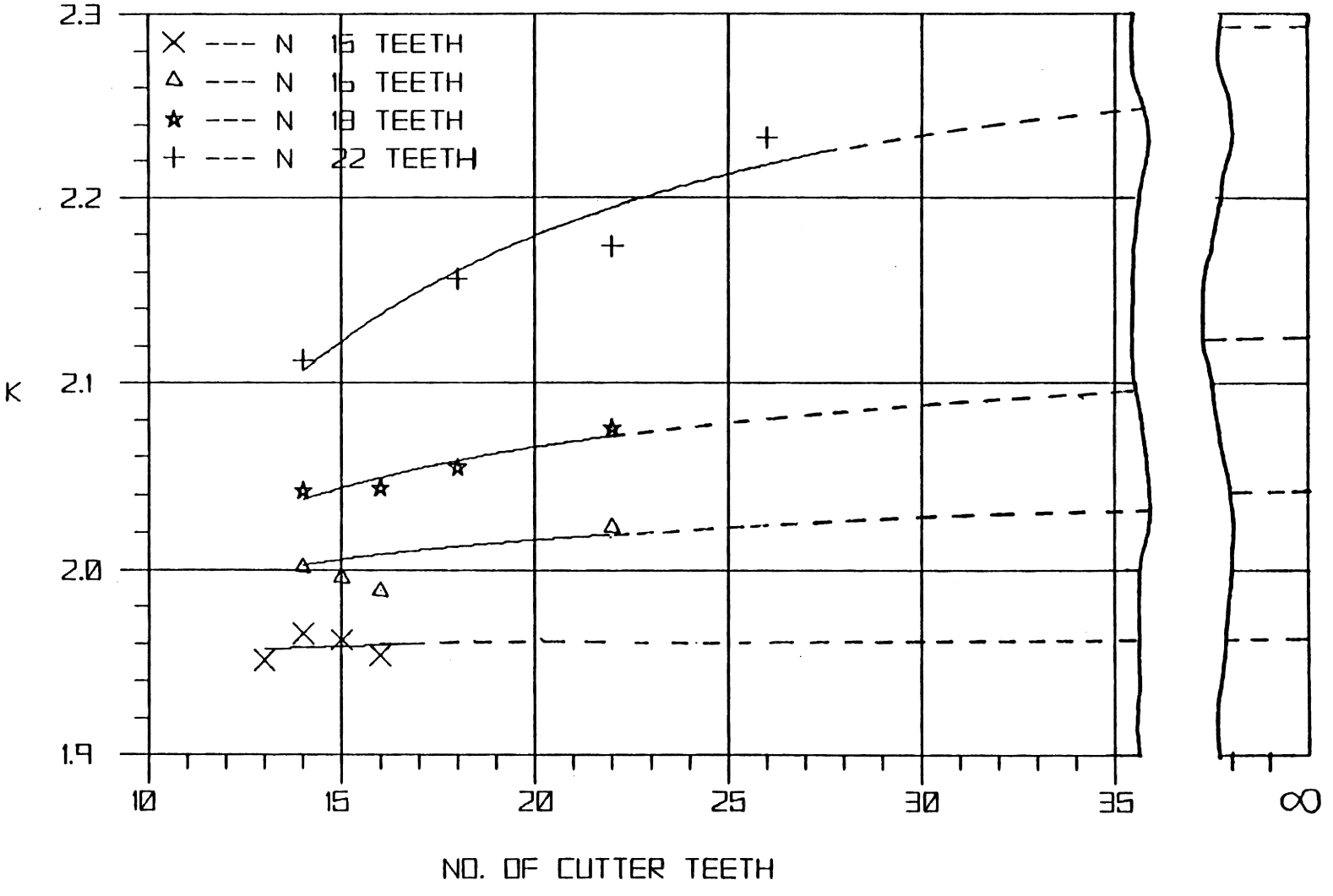

Fig. 5.4 Variation of stress concentration factor versus the number of cutter teeth (b = 1.2 in)

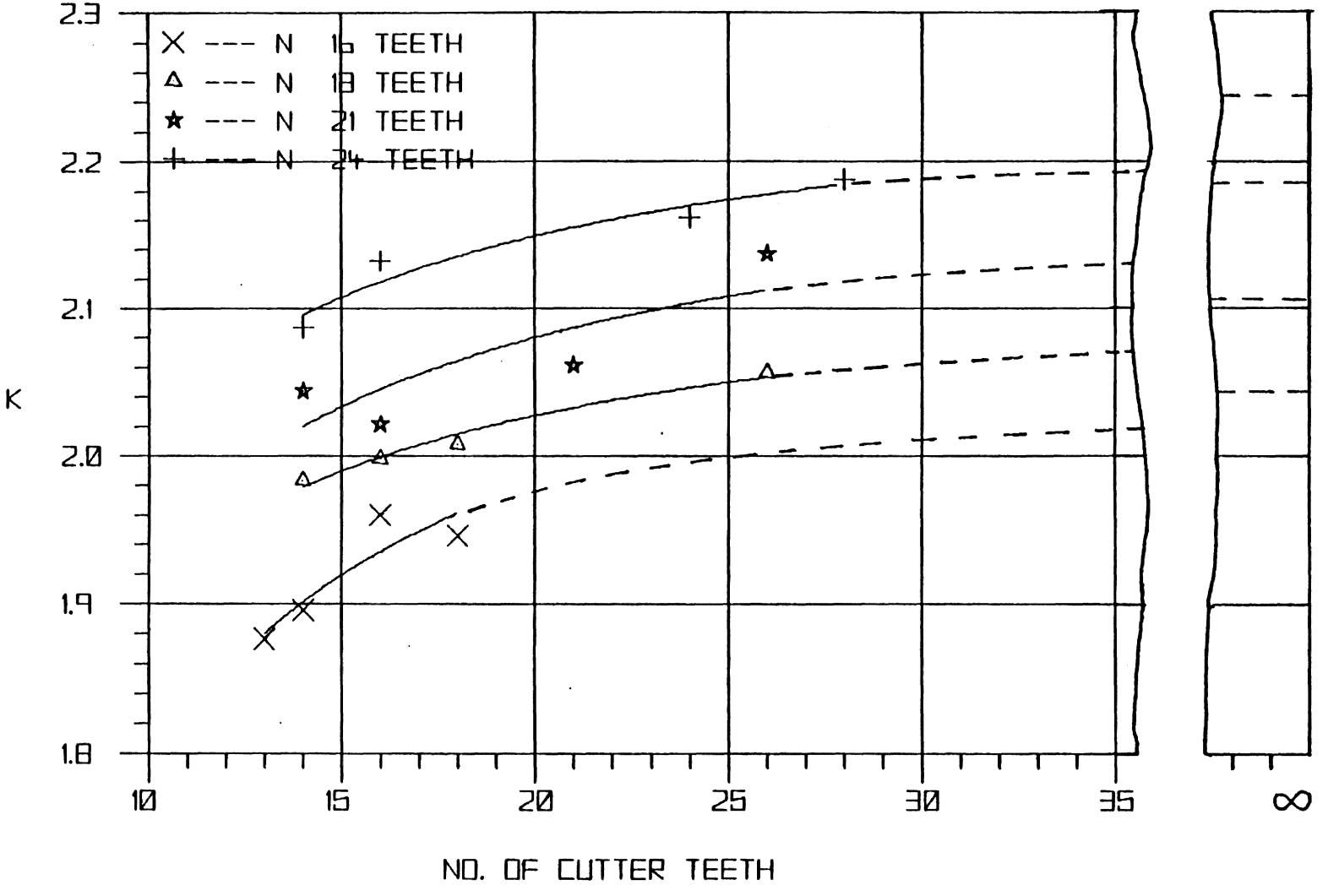

Fig. 5.5 Variation of stress concentration factor versus the number of cutter teeth (b = 1.25 in)

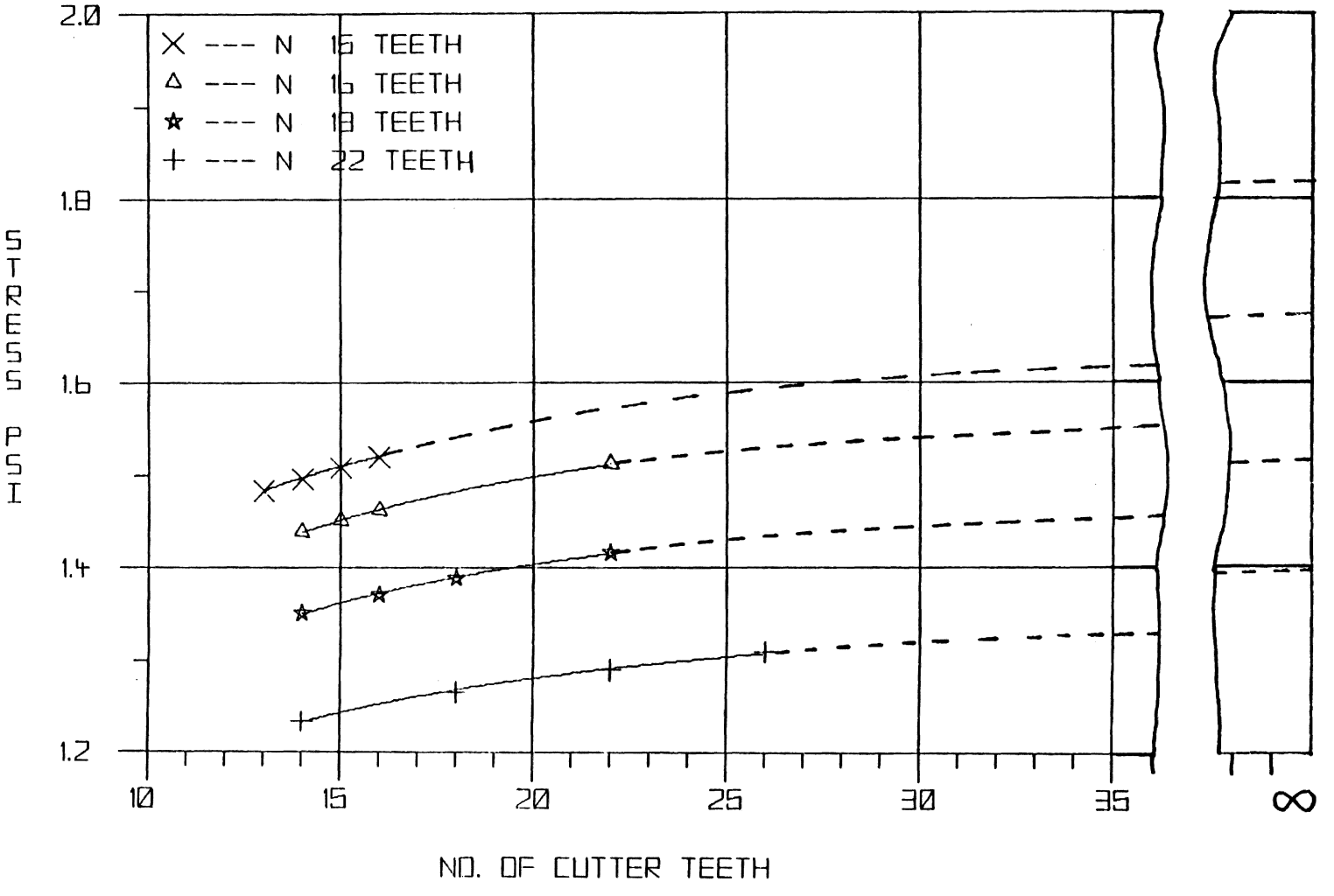

Fig. 5.6 Variation of Lewis tensile stress versus the number of cutter teeth (b = 1.2 in)

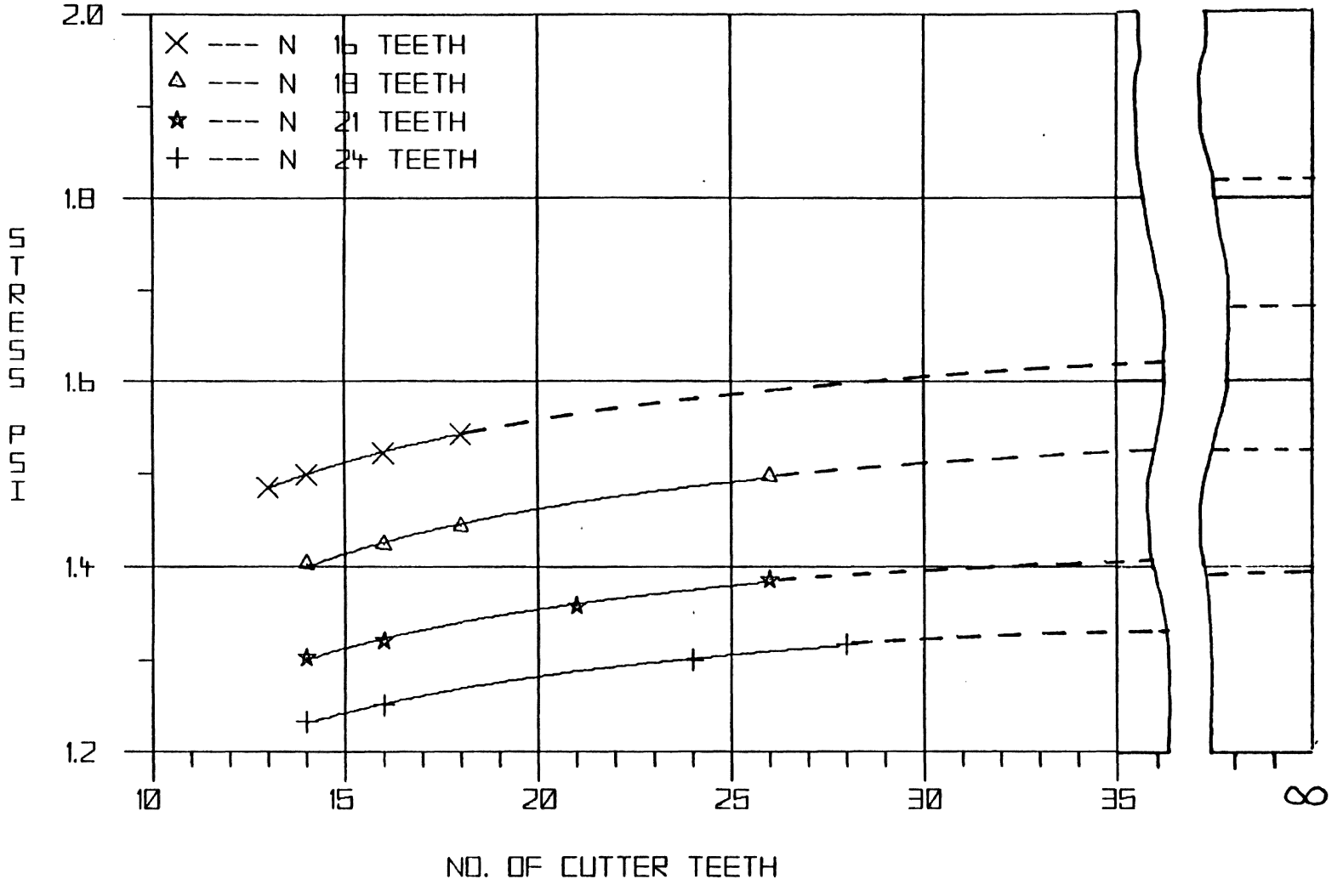

Fig. 5.7 Variation of Lewis tensile stress versus the number of cutter teeth (b = 1.25 in)

It was also necessary to determine the dependence of the stress concentration factor upon the number of teeth of the mating gear. Four additional models were analyzed for this purpose, having the same number of pinion teeth and cutter teeth. Table 5.3 lists the four models used to examine the dependence of K upon N_m and the results.

Table 5.3

Results of special study

Model	N_p	N_c	N_m	σ_T psi	K FEM
C1	18	16	20	2.7962	2.0432
C2	18	16	30	2.7286	2.1129
C3	18	16	50	2.6387	2.1715
C4	18	16	80	2.6338	2.2606

Conclusions and Recommendations

Using the results obtained from the finite element analyses, a multiple regression analysis was performed. The resulting empirical relationship (6.1) gives the stress conentration factor K_R as a function of the pinion dedendum b, the number of teeth on the pinion N_p, the number of teeth on the pinion cutter N_c, and the number of teeth on the mating gear.

$$K = [.78373 + .7309*\log(N_m)]\ [-.4117*N_p*b +$$

$$7.4200*b + .49341*N_p - 7.90400] * [7.46572 +$$

$$8.83048*b + 143.84048/N_p - B4.45584*b/N_p$$

$$-242.21370/N_c + 198.46860*b/N_c + 4907.42770/N_c/N_p$$

$$-3963.7657*b/N_c/N_p] \qquad (6.1)$$

In order to check equation 6.1, stress concentration factors for all previously analyzed models (Table 5.1) were compared to stress concentration factors predicted by equation 6.1. These results are listed in Table 6.1. The percentage differences between K_R and K are computed and tabulated. The greatest variation in K_R with K was a 3.2933 difference.

Table 6.1

Results of regression analysis

Model	b	N_p	N_c	K FEM	K_R REGRESSION	% error
A1	1.2	15	13	1.9510	1.9746	1.2096
A2	1.2	15	14	1.9655	1.9746	.4630
A3	1.2	15	15	1.9617	1.9745	.6525
A4	1.2	15	16	1.9537	1.9745	1.0646
A5	1.2	16	14	2.0080	2.0027	.0949
A6	1.2	16	15	1.9953	2.0057	.5212
A7	1.2	16	16	1.9881	2.0083	1.0160
A8	1.2	16	22	2.0227	2.0190	.1329
A9	1.2	18	14	2.0422	2.0497	.3672
A10	1.2	18	18	2.0432	2.0647	1.0523
A11	1.2	18	18	2.0541	2.0764	1.0356
A12	1.2	18	22	2.0750	2.0938	.8858
A13	1.2	22	14	2.1119	2.1180	.2888
A14	1.2	22	13	2.1558	2.1690	.6122
A15	1.2	22	22	2.7840	2.2015	1.0604
A16	1.2	22	26	2.2323	2.2240	.3713

Table 6.1
continued

Model	b	N_p	N_c	K	K_R	% error
				FEM	REGRESSION	
B1	1.25	16	13	1.8766	1.8871	.5595
B2	1.25	16	14	1.8954	1.9063	.5751
B3	1.25	16	16	1.9600	1.9375	1.1430
B4	1.25	16	18	1.9461	1.9618	.3067
B5	1.25	18	14	1.9334	2.0240	2.0469
B6	1.25	18	16	1.9979	2.0510	2.6597
B7	1.25	18	18	2.0082	2.0721	2.1819
B8	1.25	18	26	2.0569	2.1238	2.2525
B9	1.25	21	14	2.0443	2.1062	2.0279
B10	1.25	21	16	2.0214	2.1284	3.2933
B11	1.25	21	21	2.0615	2.1615	2.8508
B12	1.25	21	26	2.1372	2.1882	2.1523
B13	1.25	24	14	2.0869	2.1128	1.2410
B14	1.25	24	16	2.1321	2.1314	.0328
B15	1.25	24	24	2.1614	2.1746	.6107
B16	1.25	24	28	2.1882	2.1370	0.543

In order to verify equation 6.1, a model, not among those previously analyzed, was chosen for a test. It had the following parameters: $\phi = 20^{\circ}$, a = 1.0 in, b = 1.225 in, P = 1, $N_p = 20$, $N_c = 19$, and $N_m = 21$.

First K was obtained through finite element analysis as before. Then K_R was computed with equation 6.1. The results are listed in Table 6.2. A comparison of the two numbers, indicated a - .0838% difference between K_R and K_F. Hence, it may be deduced that equation 6.1 is an accurate formula for prediction of the stress concentration in pinion shaped teeth. It should be noted, that equation 6.1 is restricted to pinions that have a = 1.0 in, $\phi = 20^{\circ}$.

The objective of this study was to determine the effects of shaping gear teeth with a pinion cutter upon the geometry and root stresses. Figures 5.2 and 5.3 show the trend in the maximum tensile stress as the numbers of teeth on the cut gear and cutter vary. For any pinion of N teeth the cutter with the fewest number of teeth will shape the strongest pinion. As the number of teeth on the cutter tends to infinity, the cutter becomes a hob, and the bending stress increases asymptotically. It should be pointed out that this statement is true only for a sharp cornered hob. A typical hob has a rounded tip with a radius of .35 in. Using equation 6.1, maximum tensile stresses were computed for the first model in each subgroup in Table 4.1. The first model in each subgroup was shaped by a cutter that had the fewest number of teeth possible to avoid undercutting. For the case of hobbing, equation 7.1 in [13] was used to compute the maximum tensile stresses

Table 6.2

Results from testing regression formula

Model	N_p	N_c	N_m	S_L	S_T	K	K_R	% error
				psi	psi	FEM	REGRESSION	
D1	20	19	21	1.3062	2.8056	2.1479	2.1497	.0838

for the first model in each subgroup. Also, stresses were calculated for the first model in each subgroup using AGMA 218.01 [2]. These results are listed in Table 6.3. As indicated in Table 6.3, neither method of shaping gives the designer any significant advantage over the other. While a small pinion with relatively few teeth will be undercut in the generation process with a hob, the maximum tensile stress does not diminish dramatically just because the teeth are undercut [13]. Small pinions generated with a pinion cutter have stresses nearly equal to those generated by a hob. There are certain instances when only a pinion cutter may be used, as in the case of teeth cut into a shaft or a gear cutdown to a shoulder.

If hobbing were a quicker, more economical way to produce external spur gears, then it would be the preferred method, as no significant advantage in strength is gained by use of a pinion cutter. A pinion cutter can produce a nonundercut pinion with fewer teeth than a hob, and will have a longer line of action and a greater contact ratio, but these are purely kinematic quantities. In itself, a pinion cutter offers no significant strength gain over a hob in generating the same pinion. Fig. 6.1 shows the superposition of two root profiles of the same pinion, one generated by a pinion cutter the other by a hob. There is only a small variation in the root form, which leads to the same conclusion, that each shaping method produces pinions of nearly equal strength.

Table 6.3

Comparison of stresses in pinion and hobbed shaped gear teeth

Model	N	b	S_{pinion}	S_{hob}	S_{AGMA}
		in	psi	psi	psi
A1	15	1.2	3.0005	3.0061	2.7771
A5	16	1.2	2.9258	2.9220	2.6842
A9	18	1.2	2.7815	2.7838	2.5361
A13	22	1.2	2.5513	2.5919	2.3342
B1	16	1.25	2.8513	2.9659	2.7721
B5	18	1.25	2.8200	2.8234	2.6145
B9	21	1.25	2.6366	2.6678	2.6445
B13	24	1.25	2.5665	2.5553	2.3246

○ LEWIS POINT

△ INVOLUTE INTERSECTION

□ ROOT CIRCLE INTERSECTION

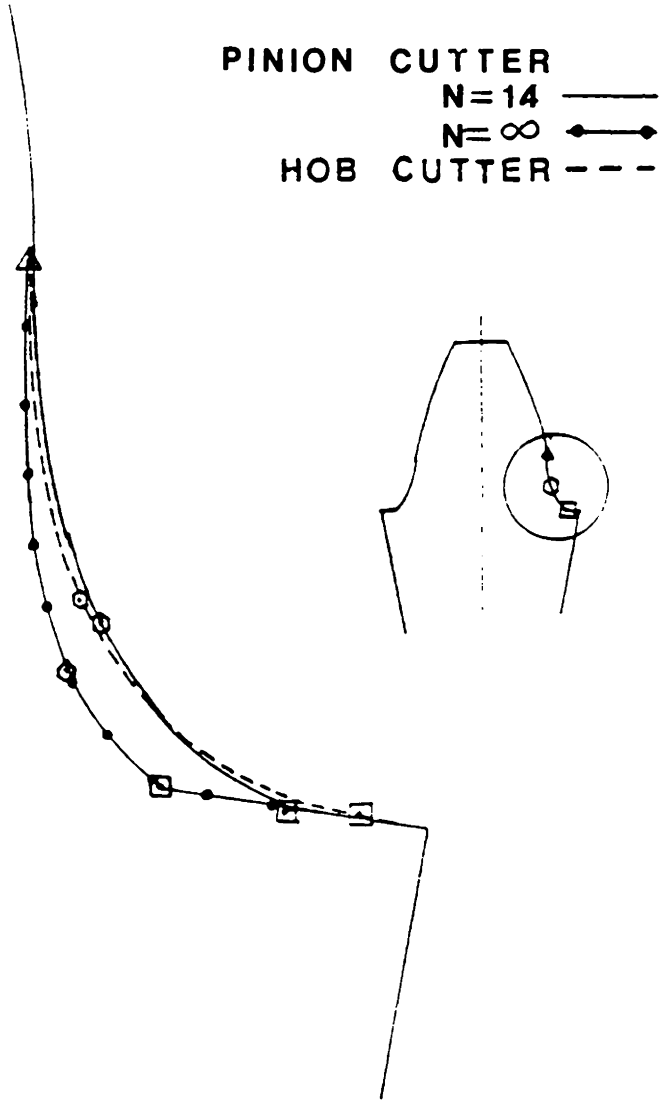

Fig. 6.1 Enlargement of the root of a pinion shaped by standard pinion and hob cutters

References

1. Shigley, J. E., Mechanical Engineering Design, Third Edition, McGraw-Hill, New York, NY, pp. 424-428, 1977.

2. American Gear Manufactures Association, AGMA Standard for Rating the Pitting Resistance and Bending Strength of Spur and Helical Involute Gear Teeth, AGMA 218.01, Arlington, VA, 1982.

3. General Electric CAE International Inc., Ideas 2.5.

4. General Electric CAE International Superb 6.0 Manual, 1983.

5. Dolan, T. J. and Broghamer, E. L., "A Photoelastic Study of Stresses in Gear Tooth Fillets", University of Illinois Engineering Experimental Station Bulletin No. 335, 1942.

6. Chaney, S. H., Huston, R. L., and Coy, J. J., "A Finite Element Stress Analysis Including Fillet Radii and Rim Thickness", NASA-TM-82865, 1982.

7. Chabert, G., Dong Tran, T., and Mathis, R., "An Evaluation of Stress and Deflection of Spur Gear Teeth Under Strain", ASME Journal of Engineering for Industry, Vol. 96, No. 1, pp. 35-93, February 1974.

8. Winter, H. and Hirt, M., "The Measurement of Actual Strains at Gear Teeth, Influence of Fillet Radius on Stress and Strength", ASME Journal of Engineering for Industry, Vol. 96, No 1. pp. 33-50, February 1974.

9. Shotter, B. A., "A New Approach to Gear Tooth Root Stress", ASME Journal of Engineering for Industry, Vol. 96, No. 1, pp. 11-18, February 1974.

10. Wilcox, L. and Coleman, W., "Application of Finite Elements for the Analysis of Gear Tooth Stresses", ASME Journal of Engineering for Industry, Vol. 95, No. 4, pp. 1139-1148, November 1973.

11. Baronet, C. N. and Tordion, G. V., "Exact Stress Distribution in Gear Teeth and Gear Roots", ASME Journal of Engineering for Industry, Vol. 95, No. 4, pp. 1159-1163, November 1973.

12. Aida, T. and Teruchic, Y., "On the Bending Stress of a Spur Gear", Bulletin of the Japanese Society of Mechanical Engineering, Vol. 5, No. 17, pp. 161-170, February 1962.

13. Jalilvand, J., "Stress Concentrations in Undercut Spur Gear Teeth Via the Finite Element Method", Master's Thesis, Virginia Polytechnic Institute and State University, Blacksburg, VA, November 1983.

14. Mitchiner, R. G. and Mabie, H. H, "The Determination of the Lewis Form Factor and the AGMA Geometry Factor for External Spur Gear Teeth", Journal of Mechanical Design, Transaction of the ASME, Vol. 104, No. 1, pp. 148-158, January 1982.

APPENDIX A

COMPUTER PROGRAM

```
      IMPLICIT REAL*8 (A-H,O-Z)
      REAL*8 N,NMATE
      REAL*4 XSNGL(3000),YSNGL(3000),ANGLE,SX,RBASE,SYMHT,SYMANG
      REAL*4 RMAXX,XMAXX,YMAXX,TX,TY,DANGLE,ADD,XPL(6),YPL(6),XXPL,YYPL
      DIMENSION X(3000),Y(3000),NPTS(9,15),NM(8)
      CHARACTER*10 FINAM
      CHARACTER*4 EXT,DAT
      CHARACTER*15 FNPNT,FNLIN,FNEDG,FNDAT
      COMMON/TOOTH/N,P,A,D,RHF,THKNSS,PHI,R,NMATE
      DATA IYES/1HY/,EXT/'.TTH'/,DAT/'.INF'/
      CALL INITT(10)
      CALL ANMODE
      PI=4.D0*DATAN(1.D0)
322   TYPE 11
11    FORMAT('  ENTER    DIAMETRAL PITCH,  ADDENDUM,  DEDENDUM',/,
     C       '           HOB TIP RADIUS,   NUMBER OF TEETH ',/)
      ACCEPT *, P,A,D,RHF,N
      TYPE 80
80    FORMAT($,' IS THIS TO BE A STANDARD GEAR <Y OR N> ? ' )
      ACCEPT 81, IRPLY
81    FORMAT(A1)
      TT=PI/(2.*P)
      WW=N/(2.*P)
      IF(IRPLY.NE.IYES) GO TO 85
      R=WW
      THKNSS=TT
      TYPE 83
83    FORMAT($,' ENTER CUTTING PRESSURE ANGLE IN DEGREES >  ')
      ACCEPT *, PHIDEG
      GO TO 84
85    CONTINUE
      TYPE 12, WW,TT
12    FORMAT(' ON CUTTING PITCH CIRCLE ENTER',/,'  CUTTING ',
     1 '  PITCH RADIUS (',F15.9,' FOR STD GEARS)',/,
     2 '  CUTTING PRESSURE ANGLE IN DEGREES',/,
     3 '  TOOTH THICKNESS (',F15.9,' FOR STD GEARS',//)
      ACCEPT *, R,PHIDEG,THKNSS
84    PHI=PHIDEG*PI/180.
C
C
```

```
      TYPE 112
112   FORMAT('  IS THIS TOOTH TO BE CUT WITH A PINION CUTTER ? <Y OR N>
     1  ',$)
      ACCEPT 81, IRPLY
      IF(IRPLY.NE.IYES) GO TO 86
C
      TYPE 113
113   FORMAT(' ENTER THE NUMBER OF TEETH IN THE CUTTER - ',$)
      ACCEPT *, NMATE
C
C
86    CONTINUE
      CALL ERASE
C
      TYPE 14, P,A,D,RHF,N,R,PHIDEG,THKNSS,NMATE
14    FORMAT('   INPUT DATA    : ',//,
     1       '  PITCH            ',F15.7,/,
     2       '  ADD. FRACTION    ',F15.7,/,
     3       '  DED. FRACTION    ',F15.7,/,
     *       '  CUTTER TIP RAD   ',F15.7,/,
     4       '  NO. OF TEETH     ',F15.7,/,
     5       '  CTG. PITCH R     ',F15.7,/,
     6       '  CTG. PR. ANG.    ',F15.7,/,
     7       '  TOOTH THKNSS     ',F15.7,/,
     8       '  NO. CUTTER TEETH ',F15.7,////,
     9    '  ENTER THE NO OF INTERVALS PER CURVE <24 MAX - 4 MIN>'/)
      ACCEPT *, XINT
      CALL ERASE
      CALL ANMODE
      INTERVL=IFIX(SNGL(XINT)+.5)
      SPACNG=.01*((A+D)/P)
      SPMIN=.95*SPACNG
      SPMAX=1.05*SPACNG
      X(1)=0.
      Y(1)=0.
C
C       LOCATE INTERSECTION/TANGENCY POINT
C
      CALL INTERSECT(RI,XI,YI,ALPHAI,THETAI,ITER,0,IER)
C
C
      IF(IER.NE.0) TYPE 320
320   FORMAT('  CANNOT LOCATE ROOT/INVOLUTE INTERSECTION')
      IF(IER.EQ.99) TYPE 328
328   FORMAT('  LACK OF CONVERGENCE IN 2000 ITERATIONS')
      IF(IER.EQ.1) TYPE 329
```

```
329   FORMAT('  POINT OF INTERSECTION NOT LOCATED PAUSIBLY')
      IF(IER.EQ.1) GO TO 322
      IF(IER.EQ.0) TYPE 331, XI,YI,RI,ITER
331   FORMAT('  INTERSECTION POINT LOCATED AT (',F12.8,' ,',F12.8,' )',/,
     1       '     AT RADIUS OF ',F12.8,/,
     2       '     POINT LOCATED IN ',I5,' ITERATIONS.')
C
C
      TYPE 133,THETAI
 133  FORMAT('  THETA @ INTERSECTION = ',F12.8)
      TYPE 135,ALPHAI
 135  FORMAT('  ALPHA @ INTERSECTION = ',F12.8,///)
C
C     LOCATE LEWIS POINT
C
330   CALL POINT(RLEWIS,XLEWIS,YLEWIS,TOUT,ITER,0,YI,IER,RC)
C
      IF(IER.NE.0) TYPE 420
420   FORMAT('  CANNOT LOCATE LEWIS POINT')
      IF(IER.EQ.99) TYPE 428
428   FORMAT('  LACK OF CONVERGENCE IN 2000 ITERATIONS')
      IF(IER.EQ.1) TYPE 429
429   FORMAT('  LEWIS POINT NOT LOCATED PLAUSIBLY')
      IF(IER.EQ.1) GO TO 322
      IF(IER.EQ.0) TYPE 430, XLEWIS,YLEWIS,RLEWIS,TOUT,ITER,RC
430   FORMAT('  LEWIS POINT LOCATED AT (',F12.8,' ,',F12.8,' )',/,
     1       '     AT RADIUS OF ',F12.8,' AND THETA OF ',F12.8,/,
     2       '     LEWIS POINT LOCATED IN ',I5,' ITERATIONS.',
     3       '     RC =  ',E12.5)
C
C
C       ANGLE OF LINE OF ACTION FOR SINGLE TOOTH LOADING.
C
C
      TEMP=DATAN(SQRT(1.-(R*DCOS(PHI)/(R+A))**2)/(R*DCOS(PHI)/(R+A)))
      PHIL=TEMP-PI/(2.*N)-XINV(TEMP)+XINV(PHI)
      PHILDEG=PHIL*180./PI
      TYPE 431,  PHILDEG
431   FORMAT('  PHIL = ',F12.6,' DEGREES')
C
C
C       STRESS AT LEWIS POINT
C
C
      WLOAD=1.*DCOS(PHIL)
      HEIGHT=RC-YLEWIS
```

```
      TYPE 432, HEIGHT
432   FORMAT('  LEWIS HEIGHT = ',F12.6,' INCHES')
      THICKNS=2.*XLEWIS
      TYPE 433, THICKNS
433   FORMAT('  LEWIS THICKNESS = ',F12.6,' INCHES')
      STRESS=6.*WLOAD*HEIGHT/THICKNS**2
      SIGMA=STRESS-WLOAD*DTAN(PHIL)/THICKNS
      TYPE 434, STRESS, SIGMA
434   FORMAT('  BENDING STRESS (UNIT LOAD)  = ',F12.6,' PSI',/,
     1       '  COMBINED STRESS (UNIT LOAD) = ',F12.6,' PSI')
C
C
C
C       DEVELOP ROOT CIRCLE
C
      IF(NMATE.NE.0) GO TO 123
      DELTA=((PI/P-THKNSS)/2.)-(D/P-RHF/P)*DTAN(PHI)-RHF/(P*DCOS(PHI))
      ETA=DELTA/R
      BETA=PI/N-ETA
      XE=(R-D/P)*DSIN(BETA)
      YE=(R-D/P)*DCOS(BETA)
      GO TO 124
123   CALL EPICY(XE,YE,0.D0)
124   XS=(R-D/P)*DSIN(PI/N)
      YS=(R-D/P)*DCOS(PI/N)
      XL=DSQRT((XS-XE)**2+(YS-YE)**2)
      BETA=PI/N-DATAN(XE/YE)
      LL=IFIX(SNGL(XL/SPACNG))
      IF(LL.EQ.0) LL=1
      IF(LL.GT.INTERVL) LL=INTERVL
      DEL=23./24.*BETA/DBLE(FLOAT(LL))
      TH=PI/N+DEL
      DO 120 I=2,3000
      TH=TH-DEL
      X(I)=(R-D/P)*DSIN(TH)
      Y(I)=(R-D/P)*DCOS(TH)
      IF(X(I).LE.XE) GO TO 121
120   CONTINUE
121   X(I)=XE
      Y(I)=YE
      IDEDTROCH=I
      NN=I+1
      DEL=.01
C
C     TROCHOID OR EPICYCLOID
C
```

```
      SPMINN=SPMIN
      SPMAXX=SPMAX
65    NNN=NN
      NTROCHPT=0
      DO 60 I=NNN,3000
      NTROCHPT=NTROCHPT+1
61    CONTINUE
      IF(I.NE.NNN) TH=TH+DEL
      IF(I.EQ.NNN) TH=DEL
      IF(NMATE.EQ.0.) CALL TROCH(X(I),Y(I),TH)
      IF(NMATE.NE.0.) CALL EPICY(X(I),Y(I),TH)
      XX=X(I)-X(I-1)
      YY=Y(I)-Y(I-1)
      SP=DSQRT(XX*XX+YY*YY)
      IF(SP.GE.SPMINN.AND.SP.LE.SPMAXX) GO TO 63
      DELOLD=DEL
      IF(SP.GT.SPMAXX) DEL=.99*DEL
      IF(SP.LT.SPMINN) DEL=1.01*DEL
      TH=TH-DELOLD
      GO TO 61
C
63    RM=DSQRT(X(I)**2+Y(I)**2)
      IF(RM.GE.RI.AND.NTROCHPT.LE.INTERVL) GO TO 70
      IF(RM.LT.RI) GO TO 60
      SPMAXX=SPMAXX*1.1
      SPMINN=SPMAXX*.9
      GO TO 65
60    CONTINUE
70    X(I)=XI
      Y(I)=YI
      ITROCHINV=I
      NN=I+1
      DEL=.01
      ALPHA=ALPHAI
      RO=R+A/P
C
C     INVOLUTE
C
      SPMAXX=SPMAX
      SPMINN=SPMIN
170   NNN=NN
      NINVPT=0
      ALPHA=ALPHAI-DEL
      DO 10 I=NNN,3000
      NINVPT=NINVPT+1
161   CONTINUE
```

```
      ALPHA=ALPHA+DEL
      CALL INVOL(X(I),Y(I),ALPHA)
      XX=X(I)-X(I-1)
      YY=Y(I)-Y(I-1)
      SP=DSQRT(XX*XX+YY*YY)
      IF(SP.GE.SPMINN.AND.SP.LE.SPMAXX) GO TO 163
      ALPHA=ALPHA-DEL
      IF(SP.GT.SPMAXX) DEL=.99*DEL
      IF(SP.LT.SPMINN) DEL=1.01*DEL
      GO TO 161
C
163   RM=DSQRT(X(I)**2+Y(I)**2)
      IF(RM.GE.RO.AND.NINVPT.LT.INTERVL) GO TO 20
      IF(RM.LT.RO) GO TO 10
      SPMAXX=SPMAXX*1.1
      SPMINN=SPMAXX*.9
      GO TO 170
10    CONTINUE
20    NN=I-1
      IINVADD=I-1
      NNX=NN
C
C       DEVELOP ADDENDUM CIRCLE
C
      PHIA=DACOS(R/(R+A/P)*DCOS(PHI))
      TO=(R+A/P)*(THKNSS/(2.*R)+XINV(PHI)-XINV(PHIA))
      BETA=TO/(R+A/P)
      LL=IFIX(SNGL(TO/SPACNG))
      IF(LL.EQ.0) LL=1
      IF(LL.GT.INTERVL) LL=INTERVL
      DEL=1.001*BETA/FLOAT(LL)
      TH=BETA+DEL
      DO 270 I=NN,3000
      TH=TH-DEL
      X(I)=(R+A/P)*DSIN(TH)
      Y(I)=(R+A/P)*DCOS(TH)
      IF(X(I).LE.0) GO TO 271
270   CONTINUE
271   X(I)=0.
      Y(I)=R+A/P
      NN=I
      IEND=I
C
C
C         STRESS CONCENTRATION FACTOR
C
```

```
      DBH=.32545455-.41669658*PHI
      DBL=.33181818-.52087072*PHI
      DBM=.26818182+.52087072*PHI
      IF(NMATE.EQ.0) GO TO 237
      RMATE=NMATE/(2.*P)
      RE=RMATE+D/P
      B=PI/N
      PHIE=DACOS(RMATE*DCOS(PHI)/RE)
      XT=RE*DCOS(PI/(2.*NMATE)+XINV(PHI)-XINV(PHIE))
      YT=RE*DSIN(PI/(2.*NMATE)+XINV(PHI)-XINV(PHIE))
      CHI=DATAN(YT/XT)
      D1=R+RMATE
      D2=RE
      D3=RMATE
      D4=B+CHI
C
      DX=D1*DCOS(B)-D1*D2/D3*DCOS(D4)
      DY=-D1*DSIN(B)+D1*D2/D3*DSIN(D4)
      D2X=-D1*DSIN(B)+D1**2*D2/D3*DSIN(D4)
      D2Y=-D1*DCOS(B)+D1**2*D2/D3*DCOS(D4)
C
      DBR=(1+(DY/DX)**2)**(3/2)/(D2Y/D2X)
C
      GO TO 239
 237     DBR=RHF/P+(D-RHF/P)**2/(R+D/P-RHF/P)
 239  DOLANK=DBH+(THICKNS/DBR)**DBL*(THICKNS/HEIGHT)**DBM
      TYPE 436, DOLANK
436   FORMAT('  DOLAN AND BROGHAMER K = ',F12.6,///)
C
C
        XSNGL(1)=FLOAT(NN-1)
        YSNGL(1)=FLOAT(NN-1)
        DO 274 LZ=2,NN
        XSNGL(LZ)=SNGL(X(LZ))
274     YSNGL(LZ)=SNGL(Y(LZ))
C
C       CLEAR SCREEN - -  DIALOG
C
      TYPE 272
272   FORMAT(///,50X,' PRESS RETURN TO CONTINUE')
      CALL ANMODE
      CALL TINPUT(IOP)
      CALL ERASE
      CALL ANMODE
C
      TYPE 273
```

```
273   FORMAT('  DO YOU WANT A SCREEN DWG OF THE TOOTH',
     C ' HALF ? <Y OR N> ',$)
      ACCEPT 81, IRPLY
      IF(IRPLY.NE.IYES) GO TO 900
C
        CALL ERASE
        CALL ANMODE
        CALL BINITT
        CALL CHECK(XSNGL,YSNGL)
        CALL DSPLAY(XSNGL,YSNGL)
        CALL TINPUT(IOP)
C
C       OUTPUT TO SDRC GRAPHICS FILES
C
900   TYPE 901
901   FORMAT('  DO YOU WANT OUTPUT TO SDRC-TYPE FILES <Y OR N> ?  ',$)
      ACCEPT 902, IRPLY
902   FORMAT(A1)
      IF(IRPLY.NE.IYES) GO TO 1000
      TYPE 906
906   FORMAT(' ENTER THE NAME OF THE FILE '
     C  ' TO BE WRITTEN - ',$)
      ACCEPT 907, FINAM
907   FORMAT(A)
      FNPNT=FINAM//EXT
      FNDAT=FINAM//DAT
      TYPE 908, FNPNT
908   FORMAT(1X,A,' CONTAINS THE POINT, CIRCLE, SPLINE, LINE DATA')
      OPEN(UNIT=21,NAME=FNPNT,TYPE='UNKNOWN')
      OPEN(UNIT=22,NAME=FNDAT,TYPE='UNKNOWN')
C
      TYPE 1300
1300  FORMAT('  ENTER RADIUS OF HOLE IN BLANK')
      ACCEPT *, HRADIUS
      TYPE 1990
1990  FORMAT('  ENTER NUMBER OF TEETH IN FE MODEL')
      ACCEPT *, XTEETH
      LTEETH=IFIX(SNGL(XTEETH+.5))
      LLTH=(LTEETH/2)*2
      IF(LLTH.EQ.LTEETH) LTEETH=LTEETH+1
C
C       GENERATE 2ND HALF OF TOOTH IN X AND Y
C
      LEND=2*IEND-3
      LL=IEND
      DO 2011 I=IEND+1,LEND
```

```
      LL=LL-1
      X(I)=-X(LL)
2011  Y(I)=Y(LL)
C
C
C       POINT FILE
C
      WRITE(21,903)
903   FORMAT('    -1',/,'    25')
C
      IPTNUM=1
      ZETA=2.*PI/N
      XI=DBLE(FLOAT((LTEETH/2)))*ZETA+ZETA
C
C
      DO 2101 I=1,LTEETH
      XI=XI-ZETA
      DO 2200 J=2,LEND
      IPTNUM=IPTNUM+1
      XNEW=Y(J)*DSIN(XI)+X(J)*DCOS(XI)
      YNEW=Y(J)*DCOS(XI)-X(J)*DSIN(XI)
      WRITE(21,2210) IPTNUM,XNEW,YNEW
2210  FORMAT(I10,9X,'0',19X,'8',2E13.5,10X,'0.0')
      IF (I.NE.1.AND.J.NE.2) GO TO 2200
      X6=0.0
      Y6=-DSQRT(XNEW**2+YNEW**2)
2200  CONTINUE
2101  CONTINUE
      XI=DBLE(FLOAT((LTEETH/2)))*ZETA+PI/N
      XNEW=(R-D/P)*DSIN(-XI)
      YNEW=(R-D/P)*DCOS(-XI)
      IPTNUM=IPTNUM+1
      WRITE(21,2210) IPTNUM,XNEW,YNEW
      WRITE(21,909)
909   FORMAT('    -1')
C
C       SPLINE FILE
C
      WRITE(21,1200)
1200  FORMAT('    -1',/,'    28')
      NM(1)=(IDEDTROCH-2)+1
      NM(2)=(ITROCHINV-IDEDTROCH)+1
      NM(3)=(IINVADD-ITROCHINV)+1
      NM(4)=(IEND-IINVADD)+1
      NPTS(1,1)=2
      NPTS(2,1)=IDEDTROCH
```

```
      NPTS(3,1)=ITROCHINV
      NPTS(4,1)=IINVADD
      NPTS(5,1)=IEND
      NPTS(6,1)=IEND+NM(4)-1
      NPTS(7,1)=IEND+NM(4)+NM(3)-2
      NPTS(8,1)=IEND+NM(4)+NM(3)+NM(2)-3
      NPTS(9,1)=IEND+NM(4)+NM(3)+NM(2)+NM(1)-4
      NM(5)=NM(4)
      NM(6)=NM(3)
      NM(7)=NM(2)
      NM(8)=NM(1)
      DO 3000 I=2,15
      DO 3001 J=1,9
      NPTS(J,I)=NPTS(J,I-1)+2*IEND-4
3001  CONTINUE
3000  CONTINUE
C
      DO 3010 J=1,LTEETH
      DO 3020 I=1,8
      LABEL=(J-1)*8+I
      WRITE(21,3030) LABEL,NM(I)
3030  FORMAT(I10,9X,'1',9X,'8',9X,'1',I10)
      WRITE(21,3040) (L,L=NPTS(I,J),NPTS(I+1,J))
3040  FORMAT(8I10)
3020  CONTINUE
3010  CONTINUE
      WRITE(21,909)
C
C      POINT FILE FOR HOLE & LINE OF ACTION
C
      WRITE(21,903)
      XI=DBLE(FLOAT((LTEETH/2)))*ZETA+PI/N
      X1=0.
      Y1=HRADIUS
      X2=HRADIUS*DSIN(XI)
      Y2=HRADIUS*DCOS(XI)
      X3=HRADIUS*DSIN(-XI)
      Y3=HRADIUS*DCOS(-XI)
      X4=0.0
      Y4=RC
      X5=2.0*DCOS(PHIL)
      Y5=2.*DSIN(PHIL)+RC
      X7=0.0
      Y7=-Y1
      N1=NPTS(9,LTEETH)+1
      N2=N1+1
```

```
      N3=N2+1
      N4=N3+1
      N5=N4+1
      N6=N5+1
      N7=N6+1
      WRITE(21,2210) N1,X3,Y3
      WRITE(21,2210) N2,X1,Y1
      WRITE(21,2210) N3,X2,Y2
      WRITE(21,2210) N4,X4,Y4
      WRITE(21,2210) N5,X5,Y5
      WRITE(21,2210) N6,X6,Y6
      WRITE(21,2210) N7,X7,Y7
      WRITE(21,909)
C
C     CIRCLE FILE FOR HOLE
C
      WRITE(21,1400)
1400  FORMAT('    -1',/,'    27',/,9X,'1',9X,'1',9X,'8',9X,'1')
      WRITE(21,1410) N1,N2,N3
1410  FORMAT(3I10)
      WRITE(21,1401)
1401  FORMAT(9X,'2',9X,'1',9X,'8',9X,'1')
      WRITE(21,1410) N3,N7,N1
      WRITE(21,1402)
1402  FORMAT(9X,'3',9X,'1',9X,'8',9X,'1')
      WRITE(21,1411) N6,NPTS(9,LTEETH)
1411  FORMAT(9X,'2',2I10)
      WRITE(21,909)
C
C       LINE FILE
C
      WRITE(21,913)
913   FORMAT('    -1',/,'    26')
      WRITE(21,914) NPTS(9,LTEETH),N1
914   FORMAT(9X,'1',9X,'8',9X,'1',2I10)
      WRITE(21,915) N3
915   FORMAT(9X,'2',9X,'8',9X,'1',9X,'2',I10)
      WRITE(21,916) N4,N5
916   FORMAT(9X,'3',9X,'8',9X,'1',2I10)
      WRITE(21,909)
C
C       DATA FILE
C
      WRITE(22,930) P,A,D,RHF,N,R,PHIDEG,THKNSS,NMATE,XLEWIS,YLEWIS,
     1   RC,PHILDEG,STRESS,SIGMA,DOLANK,SPACNG
930   FORMAT('   INPUT DATA : ',//,
```

```
     1    '  PITCH          ',F15.8,/,
     2    '  ADD. FRACTION  ',F15.8,/,
     3    '  DED. FRACTION  ',F15.8,/,
     *    '  HOB TIP RAD    ',F15.8,/,
     4    '  NO. OF TEETH   ',F15.8,/,
     5    '  CTG. PITCH R   ',F15.8,/,
     6    '  CTG. PR. ANG.  ',F15.8,/,
     7    '  TOOTH THKNSS   ',F15.8,/,
     8    '  NO OF CUTTER TEETH ',F15.8,/,
     9    '  X LEWIS POINT  ',F15.8,/,
     1    '  Y LEWIS POINT  ',F15.8,/,
     2    '  POINT K RADIUS',F15.8,/,
     3    '  PHI(L)         ',F15.8,/,
     4    '  LEWIS STRESS   ',F15.8,/,
     5    '  COMBINED STRESS',F15.8,/,
     6    '  STRESS CONCEN.',F15.8,/,
     8    '  POINT SPACING  ',F15.8,//)
1000  CONTINUE
C
C     SCALED HARD PLOTTER OUTPUT
C
      TYPE 1001
1001  FORMAT('  DO YOU WANT SCALED PLOTTER OUTPUT ? <Y OR N> ',$)
      ACCEPT 81, IRPLY
      IF(IRPLY.NE.IYES) GO TO 1005
C
      TYPE 1002
1002  FORMAT('  HOW MANY TEETH ARE TO BE DRAWN ? ',$)
      ACCEPT *, XTEETH
      NTEETH=IFIX(SNGL(1.D0+XTEETH))
      TYPE 1003
1003  FORMAT('  WHAT MULTIPLIER (TIMES FULL SIZE) IS TO BE USED ? ',$)
      ACCEPT *, SX
      TYPE 1004
1004  FORMAT('  DO YOU WANT PITCH, AND BASE CIRCLES SHOWN ?',
     C ' <Y OR N> ',$)
      ACCEPT 81, JRPLY
C
      LEND=2*NN-2
      LL=NN
      DO 3002 I=NN+1,LEND
      LL=LL-1
      XSNGL(I)=-XSNGL(LL)
3002  YSNGL(I)=YSNGL(LL)
C
      ADD=0.
```

```
      DANGLE=FLOAT(NTEETH)/SNGL(N)*2.*SNGL(PI)
      IF(DANGLE.GT.3.143) ADD=SNGL(R+A/P)*SX
      YOFFSET=((R+A/P)*DSIN(PI/N))*SX+1.D0+ADD
      XOFFSET=3.
      IF(DANGLE.GT.1.58) XOFFSET=SX*(R+A/P)+3.
      CALL PLOTS(0,0,0)
      CALL SETMSG(0)
      CALL NEWPEN(2)
C
C       ANNOTATE PLOT
C
      CALL SYMBOL(1.,9.,.25,'SCALE',0.,5)
      CALL NUMBER(4.,9.,.25,SX,0.,2)
      CALL SYMBOL(1.,8.5,.25,'PITCH',0.,5)
      CALL NUMBER(4.,8.5,.25,SNGL(P),0.,2)
      CALL SYMBOL(1.,8.,.25,'NoPINION',0.,8)
      CALL NUMBER(4.,8.,.25,SNGL(N),0.,2)
      CALL SYMBOL(1.,7.5,.25,'NoCUTTER',0.,8)
      CALL NUMBER(4.,7.5,.25,SNGL(NMATE),0.,2)
      CALL SYMBOL(1.,7.,.25,'ADDENDUM',0.,8)
      CALL NUMBER(4.,7.,.25,SNGL(A),0.,4)
      CALL SYMBOL(1.,6.5,.25,'DEDENDUM',0.,8)
      CALL NUMBER(4.,6.5,.25,SNGL(D),0.,4)
      CALL SYMBOL(1.,6.,.25,'RoF',0.,3)
      CALL NUMBER(4.,6.,.25,SNGL(RHF),0.,4)
      CALL SYMBOL(1.,5.5,.25,'doCUTTING',0.,9)
      CALL NUMBER(4.,5.5,.25,SNGL(PHIDEG),0.,4)
      CALL SYMBOL(1.,5.,.25,'RoCUTTING',0.,9)
      CALL NUMBER(4.,5.,.25,SNGL(R),0.,6)
      CALL SYMBOL(1.,4.5,.25,'NoMATING',0.,8)
      CALL NUMBER(4.,4.5,.25,SNGL(NMATE),0.,2)
C
      CALL SYMBOL(1.,2.,.125,0,0.,-1)
      CALL SYMBOL(2.,2.,.125,'START-OF-ROOT',0.,13)
      CALL SYMBOL(1.,1.5,.125,1,0.,-1)
      CALL SYMBOL(2.,1.5,.125,'LEWIS POINT',0.,11)
      CALL SYMBOL(1.,1.,.125,2,0.,-1)
      CALL SYMBOL(2.,1.,.125,'INTERSECTION POINT',0.,18)
C
      CALL PLOT(8.5,0.,-3)   !   MOVE AND RE-ORIGIN
C
      CALL PLOT(SNGL(XOFFSET),SNGL(YOFFSET),-3)
      ANGLE=2.*SNGL(PI)/SNGL(N)
      NPLPTS=2*NN-2
C
C       SCALE THE POINT ARRAY TO DWG SIZE
```

```
C
      DO 2100 I=1,NPLPTS
      XSNGL(I+1)=SX*XSNGL(I+1)
2100  YSNGL(I+1)=SX*YSNGL(I+1)
C
C       DRAW TOOTH THEN ROTATE TOOTH THRU 2PI/N AND REDRAW
C
      DO 2010 J=1,NTEETH
C
C       PLOT TOOTH
C
      DO 2000 I=1,NPLPTS
2000  CALL PLOT(YSNGL(I+1),-XSNGL(I+1),2)
      CALL PLOT(YSNGL(NPLPTS+1),-XSNGL(NPLPTS+1),3)
      IF(J.EQ.NTEETH) GO TO 2040
C
C       ROTATE POINT ARRAY FOR NEXT TOOTH
C
      DO 2020 K=1,NPLPTS
      TX=XSNGL(K+1)
      TY=YSNGL(K+1)
      XSNGL(K+1)=TX*COS(ANGLE)-TY*SIN(ANGLE)
2020  YSNGL(K+1)=TX*SIN(ANGLE)+TY*COS(ANGLE)
2010  CONTINUE
C
C       LOCATE CENTERLINE OF TOOTH
C       AND LOAD LEWIS, START-OF-ROOT, AND INTERSECTION POINTS
C
2040  CONTINUE
C
      IF(NMATE.NE.0) CALL EPICY(XPLD,YPLD,0.0001D0)
      IF(NMATE.EQ.0) CALL TROCH(XPLD,YPLD,0.0001D0)
      XPL(1)=SNGL(XPLD)
      YPL(1)=SNGL(YPLD)
      XPL(2)=-XPL(1)
      YPL(2)=YPL(1)
      XPL(3)=SNGL(XLEWIS)
      YPL(3)=SNGL(YLEWIS)
      XPL(4)=-XPL(3)
      YPL(4)=YPL(3)
      XPL(5)=SNGL(XI)
      YPL(5)=SNGL(YI)
      XPL(6)=-XPL(5)
      YPL(6)=YPL(5)
      RMAXX=1.05*SX*SNGL(R+A/P)
      SYMHT=.15*SNGL(A/P)*SX
```

```
      DO 2012 I=1,NTEETH
      TT=FLOAT(I-1)
      SYMANG=TT*ANGLE
      DO 2013 K=1,6
      ISYM=IFIX(FLOAT(K)/2.+.6)-1
      XXPL=SX*(XPL(K)*COS(TT*ANGLE)-YPL(K)*SIN(TT*ANGLE))
      YYPL=SX*(XPL(K)*SIN(TT*ANGLE)+YPL(K)*COS(TT*ANGLE))
      CALL SYMBOL(YYPL,-XXPL,SYMHT,ISYM,SYMANG,-1)
2013  CONTINUE
C
      XMAXX=RMAXX*COS(FLOAT(I-1)*ANGLE)
      YMAXX=RMAXX*SIN(FLOAT(I-1)*ANGLE)
C
C       DRAW TOOTH CENTERLINE
C
      CALL PLOT(0.,0.,3)
2012  CALL PLOT(XMAXX,YMAXX,2)
      CALL PLOT(0.,0.,3)
C
C       DRAW PITCH AND BASE CIRCLES IF REQUESTED
C
      IF(JRPLY.NE.IYES) GO TO 1005
      NZZ=SNGL(N)
      RZZ=SNGL(R)
      CALL CIRCL(RZZ,NTEETH,NZZ,SX)
      RBASE=SNGL(R)*COS(SNGL(PHI))
      CALL CIRCL(RBASE,NTEETH,NZZ,SX)
1005  CALL ERASE
      CALL ANMODE
      TYPE 2300
2300  FORMAT('  THE VERSATEC .PLV FILES HAVE BEEN BUILT.',/,
     1       '  ISSUE THE DCL COMMAND "MCR RASM" UPON COMPLETION',/,
     2       '  OF TOOTH TO GET THE PLOT ONTO THE PLOTTER.')
      CALL PLOT(0.,0.,999)
      STOP
      END
C
      SUBROUTINE CIRCL(R,NTEETH,N,SX)
      DATA PI/3.1415927/
C
C       COMPUTE DEL ANGLE FOR .05 IN. SEGMENT
C
      DEL=.05/(SX*R)
      THETA=-PI/N-DEL
C
C       COMPUTE END VALUE OF ANGLE ACCORDING TO NO OF TEETH DRAWN
```

```
C
      ENDD=FLOAT(NTEETH)*2.*PI/N
C
C       DRAW CIRCLE
C
      DO 10 I=1,10000
      THETA=THETA+DEL
      IF(THETA.GT.ENDD) GO TO 20
      X=R*SX*COS(THETA)
      Y=R*SX*SIN(THETA)
      IF(I.EQ.1) CALL PLOT(X,Y,3)
10    CALL PLOT(X,Y,2)
20    CALL PLOT(X,Y,3)
      RETURN
      END
C
      FUNCTION XINV(X)
      REAL*8 XINV,X
      XINV=DTAN(X)-X
      RETURN
      END
C
C
C
      SUBROUTINE INTERSECT(RI,X,Y,AOUT,TOUT,ITER,IDBUG,IER)
C
C       THIS ROUTINE WILL LOCATE THE POINT OF TANGENCY OR THE POINT
C       OF INTERSECTION OF THE INVOLUTE TOOTH FLANK AND THE TROCHOIDAL
C       TOOTH ROOT FOR STANDARD OR NON-STANDARD EXTERNAL INVOLUTE
C       GEAR TEETH
C
C       ARGUMENTS:
C               RI      RADIUS OF INTERSECTION/TANGENCY POINT
C               X,Y     COORDINATES OF THE POINT OF INTERSECTION/TANGENCY
C               AOUT    ALPHA OF THE INVOLUTE @ INTERSECTION
C               TOUT    THETA OF THE TROCHOID @ INTERSECTION
C               ITER    ITERATION COUNT TO SOLUTION
C               IDBUG   0 FOR NO OUTPUT OF SUBROUTINE
C                       1 FOR OUTPUT AT EACH ITERATION
C               IER     0  FOR PLAUSIBLE OUTPUT
C                       1  FOR RI IN AN UNREASONABLE RANGE
C                       99 FOR LACK OF CONVERGENCE
C
C       SUBROUTINES CALLED:
C               DERIV,INVOL,TROCH
C
```

```
C
      IMPLICIT REAL*8 (A-H,O-Z)
      REAL*8 N,NMATE
      COMMON/TOOTH/N,P,A,D,RHF,THKNSS,PHI,R,NMATE
      IER=0
 31   ITER=0
      FACTOR=1.D0
      EPS=1.D-5
C
C       APPROXIMATE ALPHA AND THETA TO BEGIN ITERATION
C       AND SET THE HISTORY VARIABLES
C
       IF(NMATE.NE.0) GO TO 33
       TYPE 63
 63    FORMAT('  ENTER START THETA AND ALPHA')
       ACCEPT *,THETA,ALPHA
C
C      ALPHA=.3D0*(1.D0-DEXP(-((N)-20.D0)/25.D0))
C      ALPHAP=ALPHA
C      THETA=.3D0*(DEXP(-((N)-20.D0)/45.D0))
C      THETAP=THETA
      GO TO 34
C
C
 32   IF(IER.EQ.0) GO TO 33
      TYPE 12
 12   FORMAT('  ENTER INITIAL THETA AND ALPHA')
      ACCEPT *,THETA,ALPHA
      GO TO 34
C
33     THETA=.31108373+(N*-.00319967)+(NMATE*.000411459)
      ALPHA=-.01491759+(N*.00347998)-(NMATE*.00019638)
34    ALPHAP=ALPHA
      THETAP=THETA
C
C
C
C       BEGIN LOOP

C
1     CONTINUE
C
C     THIS LOOP LOCATES THE POINT OF TANGENCY OR INTERSECTION
C     BETWEEN THE INVOLUTE AND THE TROCHOID
C
      ITER=ITER+1
```

```
C
C       TEST ITERATION COUNTER FOR LACK OF CONVERGENCE
C
      IF(ITER.GT.5000) GO TO 900
C
C       SET THE FACTORS TO DAMPEN OSCILLATIONS
C
C      IF(ITER.GE.10) FACTOR=.10D0
C      IF(ITER.GE.50) FACTOR=.01D0
C      IF(ITER.GE.200) FACTOR=.001D0
C
C       GET THE DERIVATIVES OF XI-XT (F1) AND YI-YT (F2)
C       SINGLE PRECISION
C
      CALL DERIV(ALPHA,THETA,F1A,F1T,F2A,F2T)
C
C       FORM THE JACOBIAN
C
      DJAC=F1A*F2T-F2A*F1T
C
C       GET THE CURRENT LOCATIONS ON THE TROCHOID AND INVOLUTE
C
      IF(NMATE.EQ.0.) CALL TROCH(XT1,YT1,THETA)
      IF(NMATE.NE.0.) CALL EPICY(XT1,YT1,THETA)
      CALL INVOL(XI1,YI1,ALPHA)
      DTEMP1=(YI1-YT1)*F1T-(XI1-XT1)*F2T
      DTEMP2=(XI1-XT1)*F2A-(YI1-YT1)*F1A
C
C       COMPUTE THE NEWTON-RHAPSON CORRECTIONS
C
      DELA=DTEMP1/DJAC*FACTOR
      DELTH=DTEMP2/DJAC*FACTOR
      ALPHA=ALPHA+DELA
      THETA=THETA+DELTH
C
C       COMPUTE ERRRORS AND COMPARE WITH ERROR CRITERION
C
      EPSA=DABS((ALPHA-ALPHAP)/ALPHA)
      EPST=DABS((THETA-THETAP)/THETA)
C
C       IF BOTH ERRORS SMALL THEN EXIT
C
      IF(EPST.LT.EPS.AND.EPSA.LT.EPS) GO TO 3
C
C       IF DEBUG SWITCH .NE. 0 WRITE ITERATION RESULTS
C
```

```
      IF(IDBUG.NE.0) TYPE 2, ITER, ALPHA,THETA
2     FORMAT(' INTERSECT *** ITER=',I5,' ALPHA=',D15.8,' THETA=',
     C   D15.8)
      ALPHAP=ALPHA
      THETAP=THETA
C
C       DON'T LET ALPHA OR THETA GO NEGATIVE
C
      IF(ALPHA.LT.0.) ALPHA=1.D-10
      IF(THETA.LT.0.) THETA=1.D-10
C
C       START LOOP AGAIN
C
      GO TO 1
C
C       EXIT LOOP
C
3     CALL INVOL(X,Y,ALPHA)
      AOUT=ALPHA
      TOUT=THETA
      RI=SQRT(X*X+Y*Y)
      RO=R+A/P
      RMIN=R-D/P
      IER=1
      IF(RI.GE.RMIN.AND.RI.LE.RO) IER=0
      IF(IER.EQ.0)GO TO 36
C
C       LOOP FOR CONVERGENCE FAILURE
C
900   IER=99
      GO TO 31
  36  RETURN
      END
C
C
      SUBROUTINE TROCH(XTR,YTR,TH)
C
C       COMPUTE THE LOCATION OF A POINT ON THE TROCHOID (XTR,YTR)
C       GIVEN THE PARAMETER TH (THETA)

C
      IMPLICIT REAL*8 (A-H,O-Z)
      REAL*8 N,NMATE

      COMMON/TOOTH/N,P,A,D,RHF,THKNSS,PHI,R,NMATE
C
```

```
C     TROCHOID
C
      PI=4.D0*DATAN(1.D0)
      DELTA=((PI/P-THKNSS)/2.)-(D/P-RHF/P)*DTAN(PHI)-RHF/(P*DCOS(PHI))
      ETA=DELTA/R
      BETA=PI/N-ETA
      XTR=-TH*R*DCOS(BETA+TH)+(R-D*P**(-1)+P**(-1)*RHF)*
     CDSIN(BETA+TH)-P**(-1)*RHF*(TH**(-1)*R**(-1)*P**(-1)*(
     CD-RHF)*(TH**(-2)*R**(-2)*P**(-2)*(D-RHF)**2+1.)**(-.5)*
     CDSIN(BETA+TH)+(TH**(-2)*R**(-2)*P**(-2)*(D-RHF)**2
     C+1.)**(-.5)*DCOS(BETA+TH))
      YTR=TH*R*DSIN(BETA+TH)+(R-D*P**(-1)+P**(-1)*RHF)*
     CDCOS(BETA+TH)+P**(-1)*RHF*(-TH**(-1)*R**(-1)*P**(-1
     C)*(D-RHF)*(TH**(-2)*R**(-2)*P**(-2)*(D-RHF)**2+1.)**(-.5
     C)*DCOS(BETA+TH)+(TH**(-2)*R**(-2)*P**(-2)*(D-RHF)
     C**2+1.)**(-.5)*DSIN(BETA+TH))
      RETURN
      END
C
      SUBROUTINE INVOL(XINV,YINV,ALPHA)
C
C       COMPUTE THE LOCATION OF A POINT ON THE INVOLUTE (XINV,YINV)
C       GIVEN THE PARAMETER ALPHA
C
      IMPLICIT REAL*8 (A-H,O-Z)
      REAL*8 N,NMATE
      COMMON/TOOTH/N,P,A,D,RHF,THKNSS,PHI,R,NMATE
C
C     INVOLUTE
C
      XINV=R*DCOS(PHI)/DCOS(ALPHA)*DSIN(((THKNSS/2.)/R)
     C  +DTAN(PHI)-PHI-DTAN(ALPHA)+ALPHA)
      YINV=R*DCOS(PHI)/DCOS(ALPHA)*DCOS(((THKNSS/2.)/R)
     C  +DTAN(PHI)-PHI-DTAN(ALPHA)+ALPHA)
      RETURN
      END
C
      SUBROUTINE DERIVX(ALPHA,THETA,F1A,F1T,F2A,F2T)
C
C       ORIGINAL DERIV SUBROUTINE BEFORE EPICYCLOIDAL CAPABILITY ADDED
C
C       FORM F1 AS XINV-XTROCH
C            F2 AS YINV-YTROCH
C       TAKE DERIVATIVES W/R ALPHA -- F1A & F2A
C                            THETA -- F1T & F2T
C
```

```
      IMPLICIT REAL*8 (A-H,O-Z)
      REAL*8 N,NMATE
      COMMON/TOOTH/N,P,A,D,RHF,THKNSS,PHI,R,NMATE
      ALDEL=ALPHA+.001
      THDEL=THETA+.001
      CALL INVOL(XI1,YI1,ALPHA)
      CALL INVOL(XI2,YI2,ALDEL)
      CALL TROCH(XT1,YT1,THETA)
      CALL TROCH(XT2,YT2,THDEL)
      F1A=(XI2-XI1)*1000.
      F1T=-(XT2-XT1)*1000.
      F2A=(YI2-YI1)*1000.
      F2T=-(YT2-YT1)*1000.
      RETURN
      END
C
      SUBROUTINE DERIV(ALPHA,THETA,F1A,F1T,F2A,F2T)
C
C       FORM F1 AS XINV-X OF ROOT FCT
C            F2 AS YINV-Y OF ROOT FCT
C       TAKE DERIVATIVES W/R ALPHA -- F1A & F2A
C                            THETA -- F1T & F2T
C
      IMPLICIT REAL*8 (A-H,O-Z)
      REAL*8 N,NMATE
      COMMON/TOOTH/N,P,A,D,RHF,THKNSS,PHI,R,NMATE
      DATA DEL/1.D-6/
      PI=4.D0*DATAN(1.D0)
C
      ALDEL=ALPHA+DEL
      THDEL=THETA+DEL
      CALL INVOL(XI1,YI1,ALPHA)
      CALL INVOL(XI2,YI2,ALDEL)
      IF(NMATE.EQ.0.) CALL TROCH(XT1,YT1,THETA)
      IF(NMATE.EQ.0.) CALL TROCH(XT2,YT2,THDEL)
      IF(NMATE.NE.0.) CALL EPICY(XT1,YT1,THETA)
      IF(NMATE.NE.0.) CALL EPICY(XT2,YT2,THDEL)
      F1A=(XI2-XI1)/DEL
      F1T=-(XT2-XT1)/DEL
      F2A=(YI2-YI1)/DEL
      F2T=-(YT2-YT1)/DEL
      RETURN
      END
C
C
      SUBROUTINE EPICY(XEPI,YEPI,THETA)
```

```
C
C       COMPUTE THE LOCATION OF A POINT ON THE EPICYCLOIDAL
C       ENVELOPE  (XEPI,YEPI) GIVEN THE PARAMETER THETA.
C
      IMPLICIT REAL*8 (A-H,O-Z)
      REAL*8 N,NMATE,IOTA
      COMMON/TOOTH/N,P,A,D,RHF,THKNSS,PHI,R,NMATE
      PI=4.D0*DATAN(1.D0)
C
C     EPICYCLOID
C
      PR=RHF
C
C
      RMATE=NMATE/(2.*P)
C
C
      RE=RMATE+D/P-PR
      PHIE=DACOS(RMATE*DCOS(PHI)/RE)
C
      XEP=RE*(DCOS(PI/2/NMATE+XINV(PHI)-XINV(PHIE)))
      YEP=RE*(DSIN(PI/2/NMATE+XINV(PHI)-XINV(PHIE)))
C
      DEL=PR/(RMATE*DCOS(PHI))
C
      ZX=XEP*DCOS(DEL)+YEP*DSIN(DEL)
      ZY=-XEP*DSIN(DEL)+YEP*DCOS(DEL)
C
      IOTA=DATAN(ZY/ZX)
      BETA=PI/N
C
      XB=R*DSIN(BETA+THETA)
      YB=R*DCOS(BETA+THETA)
C
      XTR=(R+RMATE)*DSIN(THETA+BETA)-(RE)*DSIN(THETA*(RMATE+R)/
     &    RMATE+BETA+IOTA)
C
      YTR=(R+RMATE)*DCOS(THETA+BETA)-(RE)*DCOS(THETA*(RMATE+R)/
     &    RMATE+BETA+IOTA)
C
C
      DIS=((XB-XTR)**2+(YB-YTR)**2)**.5
      CXA=(XTR-XB)/DIS
      CYA=(YTR-YB)/DIS
C
      XEPI=XB+(PR+DIS)*CXA
```

```
      YEPI=YB+(PR+DIS)*CYA
C
      RETURN
      END
C
C
      SUBROUTINE POINT(RI,X,Y,TOUT,ITER,IDBUG,YI,IER,RC)
C
C       THIS ROUTINE WILL LOCATE THE POINT OF HIGHEST TENSILE STRESS
C       ON THE ROOT FOR STANDARD OR NON-STANDARD EXTERNAL INVOLUTE
C       GEAR TEETH
C
C       ARGUMENTS:
C               RI      RADIUS OF POINT
C               X,Y     COORDINATES OF THE POINT
C               TOUT    THETA OF THE ROOT FCT @ POINT
C               ITER    ITERATION COUNT TO SOLUTION
C               IDBUG   0 FOR NO OUTPUT OF SUBROUTINE
C                       1 FOR OUTPUT AT EACH ITERATION
C               YI      Y COORDINATE OF INTERSECTION POINT
C               IER     0  FOR PLAUSIBLE OUTPUT
C                       1  FOR RI IN AN UNREASONABLE RANGE
C                       99 FOR LACK OF CONVERGENCE
C               RC      RADIUS OF K POINT FOR SINGLE-TOOTH LOADING
C
C       SUBROUTINES CALLED:
C               DERIV,INVOL,TROCH
C
C
      IMPLICIT REAL*8 (A-H,O-Z)
      REAL*8 N,NMATE,MMATE
      COMMON/TOOTH/N,P,A,D,RHF,THKNSS,PHI,R,NMATE
 456  TYPE 100
100   FORMAT(' ENTER THE NUMBER OF TEETH IN THE MATING GEAR',/,
     1       ' ENTER ZERO (0) IF SINGLE TOOTH LOADING IS TO BE',/,
     2       ' CONSIDERED -- ',$)
      ACCEPT *, MMATE
C
      CALL ERASE
      CALL ANMODE
      IER=0
 31   ITER=0
      EPS=1.D-5
C
C       APPROXIMATE THETA TO BEGIN ITERATION
C       AND SET THE HISTORY VARIABLE
```

```
C
      IF(IER.EQ.0) GO TO 33
      TYPE 56
 56   FORMAT('  ITERATION FAILED, ENTER THETA INITIAL FOR LEWIS PT')
      ACCEPT *,THETA
      GO TO 34
C
C
CC     THETA=-.001649C1*N+.0004291*NMATE+.218458
 33   THETA=.05
C
34    THETAP=THETA
C
C       BEGIN LOOP
C
1     CONTINUE
C
C     THIS LOOP LOCATES THE POINT OF TANGENCY OR INTERSECTION
C     BETWEEN THE INVOLUTE AND THE TROCHOID
C
      ITER=ITER+1
C
C       TEST ITERATION COUNTER FOR LACK OF CONVERGENCE
C
      IF(ITER.GT.2000) GO TO 900
C
C       GET THE DERIVATIVE
C
      CALL DERIV2(THETA,FTHETA,FPRIME,RC,MMATE)
      THETAP=THETA
      THETA=THETA-FTHETA/FPRIME
C
C       COMPUTE ERROR AND COMPARE WITH ERROR CRITERION
C
      EPST=DABS((THETA-THETAP)/THETA)
C
C       IF ERROR SMALL THEN EXIT
C
      IF(EPST.LT.EPS) GO TO 3
C
C       IF DEBUG SWITCH .NE. 0 WRITE ITERATION RESULTS
C
      IF(IDBUG.NE.0) TYPE 2, ITER,THETA,EPST
2     FORMAT(' POINT *** ITER=',I5,'  THETA=',D15.8,' EPST=',D15.8)
C
C       DON'T LET THETA GO NEGATIVE
```

```
C
      IF(THETA.LT.0.) THETA=1.D-10
C
C       START LOOP AGAIN
C
      GO TO 1
C
C       EXIT LOOP
C
3     CONTINUE
      IF(NMATE.EQ.0.) CALL TROCH(X,Y,THETA)
      IF(NMATE.NE.0.) CALL EPICY(X,Y,THETA)
      TOUT=THETA
      RI=DSQRT(X*X+Y*Y)
      RO=R+A/P
      RMIN=R-D/P
C
      IF(Y.GT.YI) TYPE *,' LEWIS POINT LOCATION NOT VALID Y>YI'
      IER=1
      IF(RI.GE.RMIN.AND.RI.LE.RO) IER=0
C
      IF(IER.EQ.0) GO TO 36
C
C       LOOP FOR CONVERGENCE FAILURE
C
900   IER=99
C
      GO TO 31
C
C   THIS ROUTINE LOCATES AN INTERSECTION ON THE INVOLUTE IF IT EXISTS
C
 36   CONTINUE
      PI=4.D0*DATAN(1.D0)
      PHI=20.D0*PI/180.D0
      R1=R
      R2=MMATE/2.D0/P
      RO1=R1+A
      RO2=R2+A
      TAU=DASIN(R2*DCOS(PHI)/RO2)
      Q=DCOS(TAU+PHI)*R2/DSIN(TAU)
      RX=DSQRT(Q**2+R1**2-2.D0*Q*R1*DSIN(PHI))
      TEMP=DACOS(R1*DCOS(PHI)/RX)
      K=PI/2.D0/N-XINV(TEMP)+XINV(PHI)
      PSI=(2.D0*PI/N)-K
      ETHA=DACOS((RX**2+RO2**2-((R1+R2)**2))/(2.D0*RX*RO2))-TAU
      RC=RX*DSIN(ETHA)/DSIN(ETHA+PSI)
```

```
      RB=R1*DCOS(PHI)
      CHI=PI/2.D0/N
      ALPHA=CHI+XINV(PHI)
C
C
C
      SETA=0.D0
      EPSI=.0001
      SMAX=.5
 5    DELS=.01
      U=SETA-ALPHA
C
      A1=DCOS(U)/DSIN(U)

      B1=2.*RC/(RB*DCOS(U)*(U+ALPHA)-RB*DSIN(U))
      C1=2.*RB*(U+ALPHA)*DSIN(U)+2.*RB*DCOS(U)
      D1=RB*(U+ALPHA)*DCOS(U)-RB*DSIN(U)
C
      FX=-A1+B1-(C1/D1)
C
 6    SETA=SETA+DELS
      U=SETA-ALPHA
C
      A2=DCOS(U)/DSIN(U)
      B2=2.*RC/(RB*DCOS(U)*(U+ALPHA)-RB*DSIN(U))
      C2=2.*RB*(U+ALPHA)*DSIN(U)+2.*RB*DCOS(U)
      D2=RB*(U+ALPHA)*DCOS(U)-RB*DSIN(U)
C
      FX1=-A2+B2-(C2/D2)
      IF(ABS(FX1).GT.1.D0/EPSI) GO TO 7
      GO TO 9
 7    CONTINUE
      SETA=SETA+.01
      GO TO 5
C
 9    IF(FX*FX1) 11,13,10
 10   IF(SETA.GT.SMAX) RETURN
      FX=FX1
      GO TO 6
 11   IF(DELS-EPSI) 13,13,12
 12   SETA=SETA-DELS
      DELS=DELS/10.D0
      GO TO 6
 13   RT=RB*DSQRT(1.D0+SETA**2)
      IF(RT.GT.RO1.OR.RT.LT.RI) GO TO 19
      ATA=DATAN(SETA)
```

```
      TYPE 14, ATA
 14   FORMAT('  THE PARABOLA INTERSECTS THE INVOLUTE @ ALPHA =',F10.8)
      SETA=SETA+EPSI
 19   GO TO 5
C
C
C
      END
C
      SUBROUTINE DERIV2(THETA,FTHETA,FPRIME,RC,MMATE)
C
C
C       RC        RADIUS OF POINT K
C       MMATE     NUMBER OF TEETH IN MATING GEAR FOR LEWIS PURPOSES
C
      IMPLICIT REAL*8 (A-H,O-Z)
      REAL*8 N,MJE,MJE2,K,NMATE,MMATE
      COMMON/TOOTH/N,P,A,D,RHF,THKNSS,PHI,R,NMATE
      PI=4.D0*DATAN(1.D0)
      R1=R
      IF(MMATE.EQ.0.) GO TO 110
      R2=MMATE/(2.*P)
      RO2=R2+A
      TAU=DASIN(R2*DCOS(PHI)/RO2)
      Q=DCOS(TAU+PHI)*R2/DSIN(TAU)
      RX=DSQRT(Q**2+R1**2-2.*Q*R1*DSIN(PHI))
      TEMP=DACOS(R1*DCOS(PHI)/RX)
      K=PI/(2.*N)-XINV(TEMP)+XINV(PHI)
      PSI=(2.*PI/N)-K
      ETHA=DACOS((RX**2+RO2**2-((R1+R2)**2))/(2.*RX*RO2))-TAU
      RC=RX*DSIN(ETHA)/DSIN(ETHA+PSI)
      GO TO 120
C
C       COME HERE IF TIP LOADING IS TO BE USED
C
C
 110  RADD=R1+A/P
      TVAL=RADD**2-(R1*DCOS(PHI))**2
      PHIA=DATAN(DSQRT(TVAL)/(R1*DCOS(PHI)))
      TMV=PHIA-(PI/(2.*N)+XINV(PHI)-XINV(PHIA))
      RC=R1*DCOS(PHI)/DCOS(TMV)
C
C
C
120   DEL=.001
      THDEL=THETA+DEL
```

```
C
      IF(NMATE.NE.0.) GO TO 10
C
C     THIS SECTION FOR TROCHOID
C
      DELTA=((PI/P-THKNSS)/2.)-(D/P-RHF/P)*DTAN(PHI)-RHF/(P*DCOS(PHI))
      ETA=DELTA/R
      BETA=PI/N-ETA
      MJE=-(1.+(D-RHF)/(R*THETA)*TAN(BETA+THETA))/
     *  ((D-RHF)/(R*THETA)-TAN(BETA+THETA))
      MJE2=-(1.+(D-RHF)/(R*THDEL)*TAN(BETA+THDEL))/
     *  ((D-RHF)/(R*THDEL)-TAN(BETA+THDEL))
      CALL TROCH(XT,YT,THETA)
      CALL TROCH(XT2,YT2,THDEL)
      FTHETA=MJE+2.*(RC-YT)/XT
      FTHETA2=MJE2+2.*(RC-YT2)/XT2
      FPRIME=(FTHETA2-FTHETA)/DEL
      RETURN
C
10    CONTINUE
C
C       COME HERE IF TOOTH IS PINION CUT, EPICYCLOID
C
      CALL EPIDERIV(SLOPE,SLOPE2,THETA,DEL)
      CALL EPICY(XT,YT,THETA)
      CALL EPICY(XT2,YT2,THDEL)
      FTHETA=SLOPE+2.*(RC-YT)/XT
      FTHETA2=SLOPE2+2.*(RC-YT2)/XT2
      FPRIME=(FTHETA2-FTHETA)/DEL
      RETURN
      END
C
      SUBROUTINE EPIDERIV(SLOPE,SLOPE2,THETA,DELTH)
C
C       COMPUTE THE SLOPE OF A TANGENT TO THE EPICYCLOID
C
      IMPLICIT REAL*8 (A-H,O-Z)
      REAL*8 N,NMATE,IOTA
      COMMON/TOOTH/N,P,A,D,RHF,THKNSS,PHI,R,NMATE
      PI=4.D0*DATAN(1.D0)
C
C     EPICYCLOID DERIVATIVES
C
      PR=RHF
      RMATE=NMATE/(2.*P)
      RE=RMATE+D/P-PR
```

```
      PHIE=DACOS(RMATE*DCOS(PHI)/RE)
C
      XEP=RE*(DCOS(PI/2/NMATE+XINV(PHI)-XINV(PHIE)))
      YEP=RE*(DSIN(PI/2/NMATE+XINV(PHI)-XINV(PHIE)))
C
      DEL=PR/(RMATE*DCOS(PHI))
C
      ZX=XEP*DCOS(DEL)+YEP*DSIN(DEL)
      ZY=-XEP*DSIN(DEL)+YEP*DCOS(DEL)
C
      IOTA=DATAN(ZY/ZX)
      BETA=PI/N
C
      XB=R*DSIN(BETA+THETA)
      YB=R*DCOS(BETA+THETA)
C
      XTR=(R+RMATE)*DSIN(THETA+BETA)-(RE)*DSIN(THETA*(RMATE+R)/
     &    RMATE+BETA+IOTA)
C
      YTR=(R+RMATE)*DCOS(THETA+BETA)-(RE)*DCOS(THETA*(RMATE+R)/
     &    RMATE+BETA+IOTA)
C
C
      DIS=((XB-XTR)**2+(YB-YTR)**2)**.5
      CXA=(XTR-XB)/DIS
      CYA=(YTR-YB)/DIS
      SLOPE=-CXA/CYA
C
      DELT=DELTH
      XB=R*DSIN(BETA+THETA+DELT)
      YB=R*DCOS(BETA+THETA+DELT)
C
      XTR=(R+RMATE)*DSIN(THETA+DELT+BETA)-(RE)*DSIN((THETA+DELT)*
     1  (RMATE+R)/RMATE+BETA+IOTA)
C
      YTR=(R+RMATE)*DCOS(THETA+DELT+BETA)-(RE)*DCOS((THETA+DELT)*
     1   (RMATE+R)/RMATE+BETA+IOTA)
C
C
      DIS=((XB-XTR)**2+(YB-YTR)**2)**.5
      CXA=(XTR-XB)/DIS
      CYA=(YTR-YB)/DIS
      SLOPE2=-CXA/CYA
      RETURN
      END
```

APPENDIX B

SUPERTAB PROGRAM FILE

```
IN
FEM FT RF UN
#

NM EMG T MO
/E                              CHANGE ELEMENT AND MATERIAL
DEF                             DEFAULTS
TY
PSS PQ
A MS
MA
ST
30.0E6

.283
11.5E6



!
PH
ST


/ME E                           SET THE NUMBER OF ELEMENTS PER
KM1 ;/<                         CURVE
1
3
KM1 ;/<
2

KM1 ;/<
5
12
KM1 ;/<
6
22
KM1 ;/<
16
6
```

```
KM1 ;/<
17
8
KM1 ;/<
20
8
KM1 ;/<
21
6
KM1 ;/<
18
2
KM1 ;/<
19

KD1 ;/<
G
.9
/SA CR                          CREATE THE FIRST SUBAREA - THE
                                RING  MINUS THE THREE TEETH
KM1 ;/<
C1,C5,C2,C6

N


                                NOW CREATE THE SECOND SUBAREA
                                - THE THREE TEETH


CR

KM1 ;/<
C1,C4,C2,C7,C8,C9,C10,C11,C12,C13,C14,C15,C16,C17,C18,C19,
C20,C21,C22,C23,C24,C25,C26,C27,C28,C29,C30

N


/DO E PT OF;NO ON;E ON          DRAW THE GEOMETRY WITH ONLY
/                               NODES AND ELEMENTS TURNED ON
AU;DR                           AND GENERATE THE MESH
G
```

```
1,2
PA

NM MC DO E AL OF;NO ON
LN ON
DR                          REDRAW MESH WITH NODES & LINES
                            SO RESTRAINTS AND LOADS CAN BE
LO NF ON;RE ON;LN ON        APPLIED

/RE
#
                            TRANSFER TO FILE TRANSLATOR AND
                            WRITE THE FILE THAT WILL BE
NM FT WF                    SUBMITTED TO SUPERB
SU
ST
Y
CMP.DAT
#


AL
AL
EXIT
```

NOTE 1

Upon encountering the # sign the program file transfers control back to the user. Here the user must supply the name of the .TTH file that was created using the program in Appendix A. In order to resume program file execution a ∂ sign must be typed.

Note 2

At this point the user must select the restrained nodes with the keyboard. Next the tooth to be loaded must be magnified and redrawn to permit keyboard selection of the node to be loaded. After picking the node closest to the load line, a ∂ sign must be typed to resume program file execution.

Note 3

Here the user must respond the name of the Superb file which is to be written. After doing so a ∂ sign must be typed. The finite element model is now ready to be submitted to Superb.

The vita has been removed from the scanned document